arXiv:2402.16363v1 [cs.CL] 26 Feb 2024

LLM Inference Unveiled: Survey and Roofline Model Insights

Zhihang Yuan* [1] Yuzhang Shang* [2] Yang Zhou* [3] Zhen Dong [4] Chenhao Xue [5]
Bingzhe Wu [6] Zhikai Li [7] Qingyi Gu [7] Yong Jae Lee [8] Yan Yan [2] Beidi Chen [3]
Guangyu Sun [5] Kurt Keutzer [4]

Abstract

The field of efficient Large Language Model (LLM) inference is rapidly evolving, presenting a unique blend of opportunities and challenges. Although the field has expanded and is vibrant, there hasn't been a concise framework that analyzes the various methods of LLM Inference to provide a clear understanding of this domain. Our survey stands out from traditional literature reviews by not only summarizing the current state of research but also by introducing a framework based on roofline model for systematic analysis of LLM inference techniques. This framework enables identifying the bottlenecks in LLM deployments and provides a deeper understanding of the practical aspects on real devices, thereby informing more effective strategies for deploying LLM. Furthermore, we systematically collate the latest advancements in efficient LLM inference, covering crucial areas such as weight optimization (e.g., Knowledge Distillation and Quantization), decoding algorithm improvements (e.g., Early Exit and Mixture-of-Expert), and both hardware and system-level enhancements. Distinguished by the integration of roofline model analysis, our survey provides a comprehensive and nuanced exploration of efficient LLM inference challenges and solutions. This distinctive approach not only showcases the current research landscape but also delivers valuable insights for practical implementation, positioning our work as an indispensable resource for researchers new to the field as well as for those seeking to deepen their understanding of efficient LLM deployment. The LLM-Viewer is open-sourced.

1. Introduction

Large Language Models (LLMs) have become a cornerstone of AI advancement in recent years, reshaping the landscape of machine learning and natural language processing (NLP) [Zhao et al., 2023]. This trend can be traced to the success of revolutionary models like ChatGPT [Brown et al., 2020, Ouyang et al., 2022], which produce very human-like text through their exceptional understanding and generation abilities. Following ChatGPT, other notable LLMs such as OPT [Zhang et al., 2022], BLOOM [Scao et al., 2022], and LLaMA [Touvron et al., 2023a,c] have emerged, further solidifying the consensus that larger models often lead to enhanced capabilities. Therefore, models with tens of billions of parameters are becoming increasingly common. As a result of the vast size of these models, they present considerable inference challenges, not only for devices with limited computational capabilities, but also for the most advanced hardware. Because of their complexity and scale, as well as their energy and computational demands, these models are difficult to deploy in real-world situations. Additionally, the resource-intensive nature of these models raises concerns

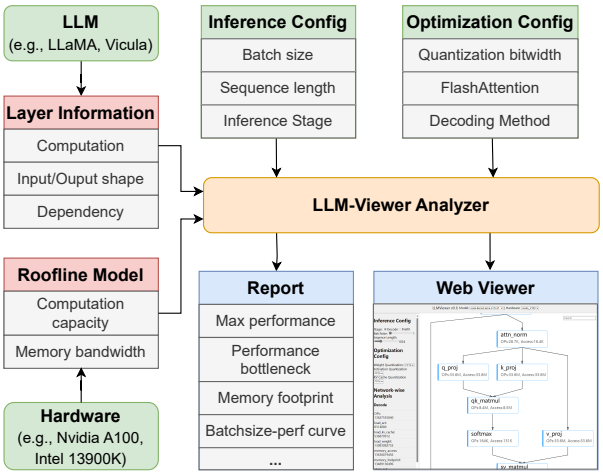

Figure 1. **Workflow of our designed LLM-Viewer.** Input: the configuration details for the intended LLM deployment and specific hardware device information. Upon receiving these inputs, the LLM-Viewer is designed to precisely analyze and identify the bottlenecks associated with deploying the given LLM on the specified hardware device, facilitating targeted optimizations for efficient LLM inference.

*Equal contribution. [1]Houmo AI. [2]Illinois Institute of Technology. [3]Carnegie Mellon University. [4]University of California, Berkeley. [5]Peking University. [6]Tencent AI Lab. [7]Institute of Automation, CAS. [8]University of Wisconsin–Madison. Zhihang Yuan (hahnyuan@gmail.com) is the project leader.

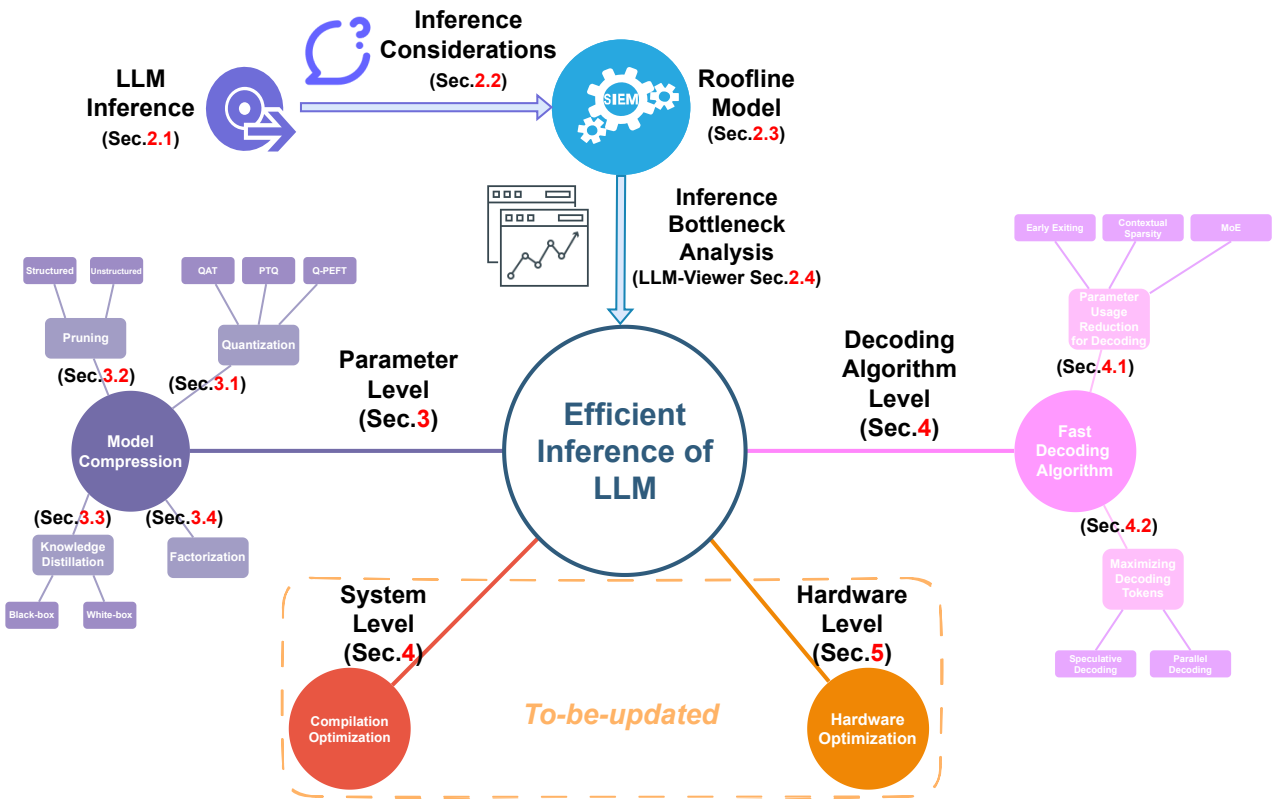

Figure 2. **Mind-map of the Survey on Efficient LLM Inference**. Our survey diverges from traditional surveys by focusing on the practical aspects of LLM inference. Specifically, we identify and analyze the challenges associated with LLM inference. Subsequently, we introduce a specially developed roofline model to pinpoint the bottlenecks in LLM inference processes (Sec.2). The survey categorizes strategies for improving LLM inference efficiency into four main areas: Parameter Reduction (Sec.3), Fast Decoding Algorithm Design (Sec.4), System-Level Optimization (to-be-updated), and Hardware-Level Optimization (to-be-updated), providing a comprehensive framework for addressing the complexities of efficient LLM deployment.

about energy consumption, scalability, and accessibility. The situation is particularly challenging for smaller organizations and communities with fewer computing resources than large corporations. Therefore, these challenges emphasize the need for innovative solutions to make LLM inference more universally accessible and sustainable.

Numerous methods have been developed to address the challenges of deploying LLM. The field of efficient LLM inference has grown exponentially in the last two years, presenting both opportunities and challenges. While the burgeoning volume of research demonstrates the field's vibrancy, it can inadvertently mask key trends and slow advancements. A critical gap in existing literature is the absence of a systematic and practical framework for unified analysis and comprehensive solution development. To bridge this gap, our work offers a comprehensive overview of the current state of research in efficient LLM inference, with a unique focus on its practice-driven characteristics. Diverging from traditional literature reviews, our work not only discusses existing research but also introduces a specifically developed roofline model. This model is designed to analyze bottlenecks in LLM deployments, a crucial step we believe is vital for practical application and optimization as shown in Figure 1. Our work is the first, to our knowledge, that provides such a tool for analyzing the intricacies of inferring LLMs on real devices, systematically collating the latest advancements in efficient LLM inference. We delve deep into deployment challenges, particularly emphasizing inference efficiency. Our discussion spans various areas, including weight optimization, decoding algorithm refinement, system-level and hardware-level enhancements, as illustrated in Figure 2. While there are concurrently related surveys in this domain, such as [Zhu et al., 2023] on LLM compression and [Miao et al., 2023a], [Ding et al., 2023] and [Wang et al., 2024] on holistic LLM serving, our work stands out by incorporating a roofline model analysis. This unique aspect allows for a more comprehensive and nuanced understanding of the challenges and solutions in efficient LLM inference, setting our work apart in its practical applicability and thoroughness.

Structure. In this paper, we first discuss the foundations of LLMs, particularly their inference and deployment

considerations (Sec.2.1-2). In contrast to traditional survey papers only focusing on literature reviews, we develop a roofline model to practically analyze the bottleneck of deploying LLMs (Sec.2.3-4). In the context of huggingface transformer[1], the most popular LLM codebase, our roofline model can be used to analyze the deployment of any LLM architecture on any hardware platform, as shown in Figure 1. Importantly, we open-source this roofline models, which can benefit the LLM community. We believe this is an important step to democratize LLM. For the literature review, this survey categorizes strategies for improving LLM inference efficiency into four main areas: Parameter Reduction (Sec.3), Fast Decoding Algorithm Design (Sec.4), System-Level Optimization (to-be-updated), and Hardware-Level Optimization (to-be-updated), providing a comprehensive framework for addressing the complexities of efficient LLM deployment.

2. Delve into LLM Inference and Deployment

Imagine a situation where your friend Alice wants to use a LLM on her personal computer to improve her novel-writing process. She needs to make a decision on which computer to purchase. How can Alice make an informed choice? Now, let's consider another scenario: Bob intends to use LLMs to offer legal document retrieval and Q&A services for his colleagues at a small company. What factors should Bob take into consideration when making a decision in this case?

In this chapter, we will delve into the details of how LLMs inference and explore the key considerations in deploying them. By the end of this chapter, you will gain a clear understanding of the operational aspects of large models and be equipped with insights to help Alice and Bob make informed decisions regarding their deployment.

2.1. LLM Inference

Nowadays, the prevailing architecture adopted by most large language models (LLMs) is the Transformer decoder architecture. Here we will provide a concise overview of its fundamental structure, with the option to refer to this survey Zhao et al. [2023] for a more in-depth understanding. This structure comprises an embedding layer, a series of sequential Transformer layers, and a prediction head. Figure 3 demonstrated the architecture.

The embedding layer transform input tokens into the hidden states. The hidden states are sent to the Transformer layers. Each Transformer layer consists of two components. Firstly, there is a masked multi-head attention module, denoted as **MHA**. Following MHA is a multi-layer perceptron submodule, labeled as **MLP**. The output from the last Transformer layer is then sent to the prediction head, which is responsible for predicting the next token after the input tokens.

Inference represents the process opposite to the training process. During training, a model learns from a vast dataset to capture the intricacies of language and context. The weights in model are updated. In contrast, during inference, a user inputs a **prompt**, and the LLM engages in a process of generating **responses**. This process involves the model utilizing its fixed pre-trained weights to comprehend the input text and produce text as output. The inference process of Large Language Models (LLMs) is divided into two stages: the **Prefill Stage** and the **Decode Stage**.

The Prefill Stage serves as the initial step in LLM inference. In this stage, the model takes a prompt sequence as input and engages in the generation of a key-value cache (KV cache) for each Transformer layer within the LLM. The KV cache plays a crucial role in storing and organizing information that the model deems relevant for subsequent token generation. Each Transformer layer is equipped with its own unique KV cache, and this prefilling process establishes the foundation for the subsequent decoding stage.

In the Prefill Stage, the Multi-Head Attention (MHA) creats key-value (KV) pairs that will be stored in the KV cache. Let's denote the input to a Transformer layer as $\mathbf{X}_{\text{pre}} \in \mathbb{R}^{n \times d}$, where d is the hidden size and n is the length of prompt token sequence. The layers in the MHA have weights represented by $\mathbf{W}_q$, $\mathbf{W}_k$, $\mathbf{W}_v$, and $\mathbf{W}_o$. The query, key and value are computed through the following process:

$$\begin{aligned} \text{Query:} \quad \mathbf{Q}_{\text{pre}} &= \mathbf{X}_{\text{pre}} \cdot \mathbf{W}_q \\ \text{Key:} \quad \mathbf{K}_{\text{pre}} &= \mathbf{X}_{\text{pre}} \cdot \mathbf{W}_k \\ \text{Value:} \quad \mathbf{V}_{\text{pre}} &= \mathbf{X}_{\text{pre}} \cdot \mathbf{W}_v \end{aligned}$$

The generated $\mathbf{K}_{\text{pre}}$ and $\mathbf{V}_{\text{pre}}$ are stored in the KV cache. The other computation in MHA can be formulated as [2]:

$$\mathbf{O}_{\text{pre}} = \text{softmax}\left(\frac{\mathbf{Q}_{\text{pre}} \cdot \mathbf{K}_{\text{pre}}^T}{\sqrt{d}}\right) \cdot \mathbf{V}_{\text{pre}} \cdot \mathbf{W}_o + \mathbf{X}_{\text{pre}},$$

where the output of MHA $\mathbf{O}_{\text{pre}} \in \mathbb{R}^{n \times d}$ is sent to the MLP. The output of the MLP serves as the input for the next Transformer layer.

The Decode Stage represents the core of the LLM inference process. In the Decode Stage, the model uses the KV caches prepared earlier and might add new information to them. The goal here is to generate tokens, which are essentially words or parts of words. This happens step by step. The creation of each new token is influenced by the tokens that were generated before it, like building a sentence word by word.

In the Decode Stage, the MHA loads the previously stored KV cache $\mathbf{K}_{\text{cache}}$ and $\mathbf{V}_{\text{cache}}$. The input is $\mathbf{X}_{\text{dec}} \in$

[1] https://huggingface.co/docs/transformers/index

[2] We omit layer norm, position mask, and positional embedding for simplicity.

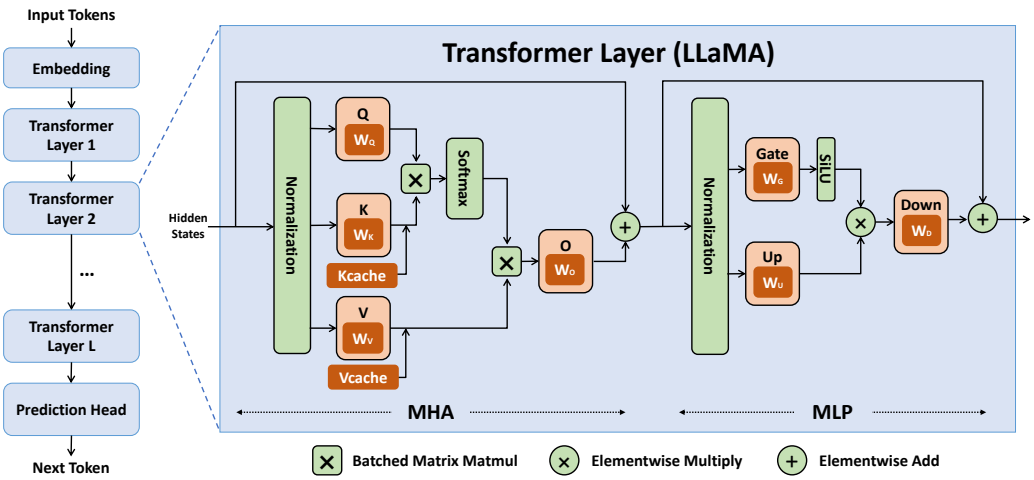

Figure 3. Demonstration of the architecture of LLMs.

$\mathbb{R}^{1\times d}$. New key and value pairs are computed and concatenated to the existing cache:

$$\begin{aligned} \text{Query:} \quad & \mathbf{Q}_{\text{dec}} = \mathbf{X}_{\text{dec}} \cdot \mathbf{W}_q \\ \text{Key:} \quad & \mathbf{K}_{\text{cat}} = [\mathbf{K}_{\text{cache}}, \mathbf{X}_{\text{dec}} \cdot \mathbf{W}_k] \\ \text{Value:} \quad & \mathbf{V}_{\text{cat}} = [\mathbf{V}_{\text{cache}}, \mathbf{X}_{\text{dec}} \cdot \mathbf{W}_v] \end{aligned}$$

These newly computed $\mathbf{X}_{\text{dec}} \cdot \mathbf{W}_k$ and $\mathbf{X}_{\text{dec}} \cdot \mathbf{W}_v$ are then appended to the KV cache. The other computation in MHA is carried out as follows:

$$\mathbf{O}_{\text{dec}} = \text{softmax}\left(\frac{\mathbf{Q}_{\text{dec}} \cdot \mathbf{K}_{\text{cat}}^T}{\sqrt{d}}\right) \cdot \mathbf{V}_{\text{cat}} \cdot \mathbf{W}_o + \mathbf{X}_{\text{dec}}$$

where the output of MHA $\mathbf{O}_{\text{dec}} \in \mathbb{R}^{1\times d}$ is sent to the MLP. The output of the last Transformer layer is sent to the final prediction layer to predict the next token.

2.2. Considerations on Deployment

In the realm of large model inference and deployment, three key factors demand our attention: the computation capability of the hardware, the size of hardware memory, and the bandwidth of that memory. These elements intertwine, playing a pivotal role in the efficiency and success of deploying large models.

Computation Capability: The heart of the matter lies in the computation capability of the hardware. First off, the hardware has to be able to handle the data flow for operations like matrix multiplication and non-linear functions (such as softmax). Also, it needs to support the data types used in these operations, like the common ones - FP16 and FP32, or even INT8 if the model is quantized. If the hardware can handle all the operations needed by the LLMs, then there's a chance it can be deployed. And don't forget, the hardware needs enough computational power, meaning it should have plenty of processing units (such as CUDA cores in GPU). We can measure the computational capability by peak computational performance (operations per second, OPS).

Memory Size: For LLMs, having sufficient memory is crucial to hold the weight of the model's parameters and intermediate results during inference. LLMs' weights can be several gigabytes (GB) to even over a hundred GB for really big models. The KV cache changes based on how much text you're working with and the size of the group of tasks you're doing (batch size). If you're dealing with a lot of text or have a big batch size, the KV cache can take up several GBs to tens of GBs of space.

Memory Bandwidth: Memory bandwidth refers to the rate at which data moves between the memory and the computation units. When data transfer is slow, the computation units have to wait idly for the data to arrive. This can pose a significant bottleneck for LLMs. In the next section, we will delve into a detailed explanation of this issue.

Choosing the right hardware for LLMs isn't a one-size-fits-all situation because of the difference of various tasks. The differences in tasks mainly come down to batch size, the ratio between the prefill and decode stages, and the length of the sequences. Take Alice, for example. She uses a single batch for her own needs and prefers long sequences for writing novels. Since her task is more focused on generating content, she needs a high ratio of the decode stage. On the other hand, Bob needs multiple batches to cater to simultaneous queries from different people in the company. As his task is more about queries and retrieval, he requires a high ratio of the prefill stage.

In the next section, we will take both the hardware and tasks into consideration and introduce how to evaluate the efficiency of inference.

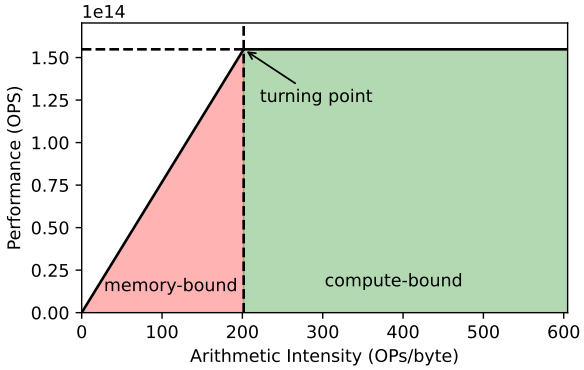

Figure 4. Demonstration of the Roofline model of Nvidia A6000 GPU. The computation is in FP16.

2.3. Roofline Model

Assessing the efficiency at which LLMs deploy onto specific hardware involves a comprehensive consideration of both hardware and model characteristics. To conduct this evaluation, we employ a technique known as the Roofline model. The Roofline model serves as an effective theoretical framework to assess the potential performance of deploying a model on particular hardware.

The execution of a neural network layer on hardware devices entails the transfer of data from memory (DDR or HBM) to on-chip buffers, followed by computations performed by on-chip processing units, ultimately outputting results back to memory. Therefore, evaluating performance requires simultaneous consideration of memory access and processing unit capabilities. If a layer involves extensive computations but minimal memory access, it is termed a computation bottleneck. This scenario leads to idle on the memory access. On the contrary, when a layer requires substantial memory access with fewer computational demands, it is referred to as a memory bottleneck. In this case, computational units remain underutilized. We can clearly distinguish between these two scenarios according to the Roofline model and provide performance upper bounds for different situations.

There are two steps to using the Roofline model:

1. **Plot the Roofline**: Determine the peak computational performance (operations per second, OPS) and peak memory bandwidth (bytes per second) specific to the target hardware device.[3] Then create a graph with performance (OPS) on the y-axis and arithmetic intensity (OPs/byte) on the x-axis: Draw a horizontal line equal to the peak computational performance. This line represents the maximum achievable performance by the hardware device. And draw a diagonal line from the origin with a slope equal to the peak memory bandwidth. This line represents the maximum memory bandwidth available on the system, known as the memory roofline. Figure 4 demonstrates the Roofline model of Nvidia A6000 GPU.

[3]OPS refer to the number of operations per second. Each Multiply-Accumulate (MAC) operation counts two operations.

Table 1. Analysis for layers in LLaMA-2-7b using the Roofline model of Nvidia A6000 GPU. In this example, the sequence length is 2048 and the batch size is 1.

Layer Name	OPs	Memory Access	Arithmetic Intensity	Max Performance	Bound
Prefill					
q_proj	69G	67M	1024	155T	compute
k_proj	69G	67M	1024	155T	compute
v_proj	69G	67M	1024	155T	compute
o_proj	69G	67M	1024	155T	compute
gate_proj	185G	152M	1215	155T	compute
up_proj	185G	152M	1215	155T	compute
down_proj	185G	152M	1215	155T	compute
qk_matmul	34G	302M	114	87T	memory
sv_matmul	34G	302M	114	87T	memory
softmax	671M	537M	1.25	960G	memory
norm	59M	34M	1.75	1T	memory
add	8M	34M	0.25	192G	memory
Decode					
q_proj	34M	34M	1	768G	memory
k_proj	34M	34M	1	768G	memory
v_proj	34M	34M	1	768G	memory
o_proj	34M	34M	1	768G	memory
gate_proj	90M	90M	1	768G	memory
up_proj	90M	90M	1	768G	memory
down_proj	90M	90M	1	768G	memory
qk_matmul	17M	17M	0.99	762G	memory
sv_matmul	17M	17M	0.99	762G	memory
softmax	328K	262K	1.25	960G	memory
norm	29K	16K	1.75	1T	memory
add	4K	16K	0.25	192G	memory

2. **Analyze performance for layers**: Evaluate the performance of each layer in the model by quantifying both the number of operations (OPs) and the volume of data accessed from memory (bytes). Calculate the arithmetic intensity (OPs/byte) of each layer by dividing the required operations by the amount of data transferred. According to the graph created in the first step, the theoretical max performance for each layer is determined by the position on the graph corresponding to the x-axis value of arithmetic intensity. It allows us to ascertain whether the system is memory-bound or compute-bound at this point, guiding the determination of the subsequent optimization strategy.

There are two scenarios where resources are not fully utilized: When the model's computational intensity is below the turning point, residing in the red zone, it implies that the computational workload required per memory access is low. Even saturating the peak bandwidth does not fully utilize all computational resources. In such cases, the layer is constrained by memory access (memory-bound), and some computational units may remain idle. If the layer

is memory-bound, consider optimization techniques such as quantization, kernel fusion and increasing batch size to alleviate the memory footprint. Conversely, if the model's computational intensity is above the turning point, situated in the green zone, it suggests that the model requires only a small amount of memory access to consume a significant amount of computational capability. It implies that the layer is constrained by computation (compute-bound), with some memory units potentially remaining idle. In this case, we should investigate strategies such as enabling low-bit computation to enhance computational efficiency. Detailed explanations of these methods will be provided in the subsequent sections.

As an example, Table 1 presents the analysis of layers in LLaMA-2-7b using the Roofline model on the Nvidia A6000 GPU. From the table, we observe that during the prefill stage, the majority of computations are compute-bound, leading to high performance. Conversely, in the decode stage, all computations are memory-bound, resulting in performance significantly below the computational capacity of the GPU's computation units. During the user's interaction with large models, the prefill stage executes only once, while the decode stage is repeatedly performed to generate a continuous output. Therefore, optimizing for the memory-bound characteristics of the decode stage becomes crucial for enhancing the inference performance of large models.

2.4. LLM-Viewer

There are multiple Transformer layers in LLMs, each containing various operations. Moreover, different LLMs have different sets of operations. Additionally, we need to track information like memory footprint to calculate the peak memory usage and total inference time. Hence, analyzing LLMs involves examining network-wide concerns. In this section, we propose a powerful tool, LLM-Viewer [4], to execute the network-wise analysis. It enables the analysis of LLM performance and efficiency on various hardware platforms, offering valuable insights into LLM inference and performance optimization.

The workflow of LLM-Viewer is depicted in Figure 1. It consists of the following steps: (1) Input the LLM and gather essential information about each layer, such as the computation count, input and output tensor shapes, and data dependencies. (2) Provide input for the hardware and generate a roofline model that takes into account the computation capacity and memory bandwidth of the hardware. (3) Configure the inference settings, including the batch size, prompt token length, and generation token length. (4) Configure the optimization settings, such as the quantization bitwidth, utilization of FlashAttention, decoding methods, and other system optimization techniques. (5) The LLM-Viewer Analyzer utilizes the roofline model and layer information to analyze the performance of each layer. It also tracks the memory usage of each layer and calculates the peak memory consumption based on data dependencies. By aggregating the results of all layers, the overall network performance of LLM can be obtained. (6) Generate a report that provides information such as the maximum performance and performance bottlenecks of each layer and the network, as well as the memory footprint. Analyzing curves, such as batch size-performance and sequence length-performance curves, can be plotted from the report to understand how different settings impact performance. (7) LLM-Viewer offers a web viewer that allows convenient visualization of the network architecture and analysis results. This tool facilitates easy configuration adjustment and provides access to various data for each layer.

[4]The tool is open-sourced at https://github.com/hahnyuan/LLM-Viewer

3. Model Compression

The formidable size and computational demands of Large Language Models (LLMs) present significant challenges for practical deployment, especially in resource-constrained environments. To alleviate these limitations, the most straightforward solution is to compress the LLMs. In this section, we review the concept of neural network compression for LLMs. This exploration encompasses a thorough examination of well-established techniques, including but not limited to quantization, pruning, knowledge distillation, and low-rank factorization. In each subsection, we will utilize LLM-Viewer to analyze the impact of network compression on LLM inference. Based on our analysis, we will provide optimization recommendations.

3.1. Quantization

In the realm of LLM compression, quantization has become a pivotal technique for mitigating the substantial storage and computational overhead associated with these models. Essentially, quantization involves transforming the floating-point values in original LLMs into integers or other discrete forms, a process that considerably reduces both storage requirements and computational complexity [Gholami et al., 2022]. While some degree of precision loss is inherent in this process, carefully designed quantization techniques can achieve significant model compression with minimal impact on accuracy. Quantization in the context of LLMs can be primarily categorized into two directions: Quantization for Compressing Pre-trained LLMs and Quantization for Parameter-Efficient Fine-Tuning (Q-PEFT). The first category encompasses approaches that apply quantization to LLMs for using the quantized LLMs as pre-trained models. This category can be further divided into two subcategories: Quantization-Aware Training (QAT) and Post-Training Quantization (PTQ). QAT integrates quantization into the model's training process or during the fine-tuning/re-training of a pre-trained LLM, al-

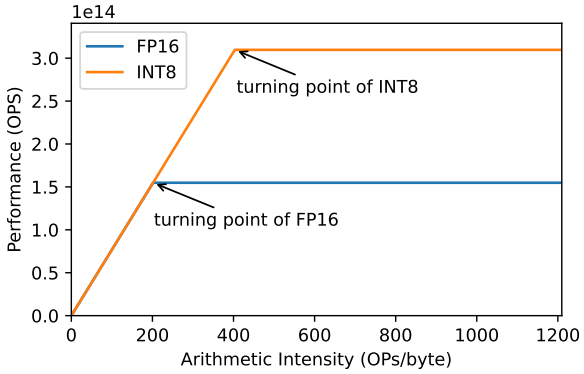

Figure 5. Demonstration of the Roofline model of Nvidia A6000 GPU for different computation data types.

lowing the model to adapt to the quantization from the onset. In contrast, PTQ applies quantization to a model after it has completed its training phase, offering a more straightforward approach to model compression without the need for retraining. These distinct methodologies highlight the versatility of quantization techniques in addressing the specific needs and constraints of LLM deployment.

3.1.1 A Use Case of LLM-Viewer: Roofline Analysis for Quantization

Here we provide an example of how to use our LLM-Viewer (Section 2.4) to analyze the bottlenecks of LLM deployments. In LLMs, tensors consist of weights and activations, with activations including temporary activations and KV cache. (1) LLM weights must be stored in memory. For example, LLaMA-13b [Touvron et al., 2023a], which has 13 billion weights, occupies approximately 26GB of memory in FP16 format. (2) temporary activations are generated during inference. For example, the inputs of each transformer layer are kept in memory until the residual addition is executed. (3) for auto-regressive LLMs, caching key and value activations (KV cache) into memory is necessary for subsequent token generation. We utilize LLM-Viewer to analyze the effects of quantization on these tensors from three perspectives: computation, memory consumption, and memory access.

Computation: The latest computing devices, such as NVIDIA GPUs, generally support FP32, FP16, and INT8 data types for computation. Hardware devices generally perform better when processing data with smaller bit widths. NVIDIA's A6000 GPU, for example, is capable of performing twice as fast as FP16 with 155 TOP/s and 310 TOP/s, respectively. In the Roofline model, when enabling quantization for faster computation, the roofline height increases, indicating improved performance for compute-bound layers. As shown in Figure 5, the max performance

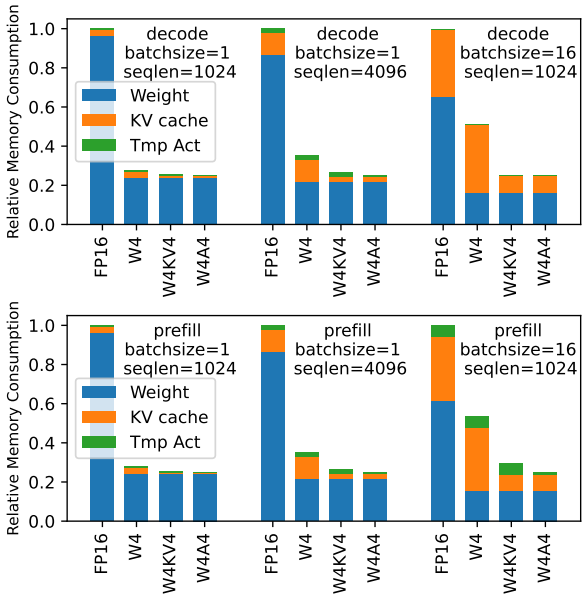

Figure 6. Relative memory consumption for different quantization settings for LLaMA-2-13b.

improved when using INT8 computation. However, to utilize the computational power of INT8, all input operands must be in INT8 format. Consequently, if only the weights are quantized to INT8 while the activations remain in FP16 format, the INT8 computational power cannot be utilized. Instead, the INT8 weights would need to be converted to FP16 for multiplication with FP16 activations. Furthermore, when tensors are quantized to a bitwidth that is not supported by the hardware, they need to be converted to higher bit widths for computation. For example, the NVIDIA H100 GPU does not support INT4 computation. Consequently, if the weight or activation is quantized to INT4, it would require conversion to a higher bit width, such as INT8 or FP16, for computation.

Memory Consumption: The memory consumption reduction resulting from quantizing different tensors varies, as shown in Figure 6 [5]. Notably, the memory usage of temporary activations is relatively low, especially during the decode stage. This can be attributed to their short lifespan, allowing their memory to be released once their purpose is fulfilled. On the other hand, the memory allocated for the KV cache behaves differently. It cannot be freed until the entire process of generating a complete answer is finished, which entails multiple inference passes through the network. Additionally, the memory consumption of the KV

[5] In our notation, W4 represents the quantization of weights to 4 bits while keeping activations in FP16 format. W4A4 indicates both weights and activations quantized to 4 bits. In the case of W4KV4, weights and the KV cache are quantized, while temporary activations remain in FP16 format.

cache increases as the batch sizes grow larger and the input sequences become longer. This is because the model needs to store a greater number of key-value (KV) pairs to facilitate its operations.

Memory Access: Quantizing tensors in LLM can significantly reduce memory access, resulting in fewer data bytes to be moved for the same amount of computation. This increase in arithmetic intensity contributes to the Roofline model, leading to three scenarios: (1) After quantization, the arithmetic intensity remains within the memory-bound range. With the improvement in arithmetic intensity, the average data access per computation is reduced, alleviating the pressure on data memory access. Consequently, the theoretical performance is enhanced. This can greatly boost the performance during the memory-bound decode stage. (2) The arithmetic intensity transitions from being memory-bound to compute-bound. This shift also reduces the pressure on data memory access, resulting in improved theoretical performance. (3) Both before and after quantization, the arithmetic intensity remains within the compute-bound range. In this case, there is no performance improvement. For example, this scenario can occur during the compute-bound prefill stage or when the batch size is large in the decode stage.

As depicted in Figure 7, when the batch size is small, the layers in the network are memory-bound both before and after quantization. Therefore, quantization can enhance performance and reduce the network's inference time. However, when the batch size is large, compressing the network's weights from 4 bits to 2 bits or 1 bit does not lead to a decrease in the inference time. This is because, at this point, the network is already compute-bound, and quantizing the weights becomes ineffective. Similar to the previous scenario, the behavior of the system can exhibit saturation effects in prefill stage. As shown in Figure 8, when the sequence length is relatively small, the prefill stage is memory-bound. In this case, applying quantization can enhance the performance by reducing the memory access requirements of the network. However, as the sequence length increases, the prefill stage becomes more compute-bound. Consequently, quantizing the weights may not yield significant improvements in performance when the network is already compute-bound during the prefill stage with large sequence lengths.

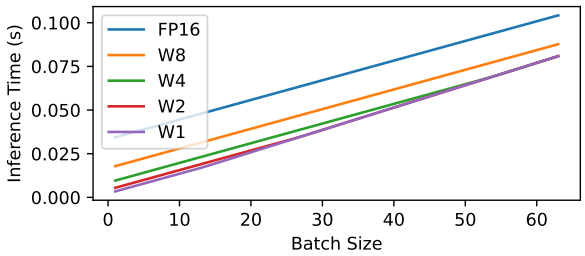

Figure 7. Inference time of decoding stage for different quantization settings on LLaMA-2-13b. (Sequence length=1024)

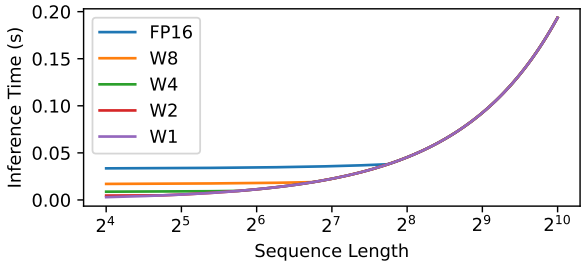

Figure 8. Inference time of prefill stage for different quantization settings on LLaMA-2-13b. (Batch size=1)

3.1.2 Quantization for Compressing Pre-trained LLMs

In Quantization-Aware Training (QAT) [Choi et al., 2018, Courbariaux et al., 2015, Dong et al., 2019], the quantization process is seamlessly integrated into the training of Large Language Models (LLMs), enabling them to adapt to low-precision representations and thus mitigating precision loss. LLM-QAT [Liu et al., 2023b] innovatively addresses the challenge of training data acquisition for LLMs through data-free distillation, which leverages outputs from a pre-trained model to obviate the need for extensive data collection. Furthermore, LLM-QAT expands quantization beyond weights and activations to include key value (KV) caches, enhancing throughput and supporting longer sequence dependencies. Its successful distillation of large LLaMA models to 4-bit quantized weights and KV caches underscores the potential for accurately quantized 4-bit LLMs.

To attain lower-bit quantization, such as below 2-bit, Kim et al. [2023b] introduce Token-Scaled Logit Distillation (TSLD) for ternary QAT in LLMs. This method employs an adaptive knowledge distillation technique that modifies Logit Knowledge Distillation based on token confidence, providing tailored guidance during LLM QAT. Furthermore, Shang et al. [2023] focus on salient weights with their concept of partially binarized matrices in PB-LLM. By preserving these crucial weights in higher bits, PB-LLM effectively maintains the reasoning capacity of heavily quantized LLMs. Additionally, PB-LLM explores minimizing quantization error by determining the optimal scaling factors for binarized LLMs, a vital step in preserving the effectiveness of models under aggressive quantization.

Post-Training Quantization (PTQ)

Post-Training Quantization (PTQ) represents a crucial technique in optimizing Large Language Models (LLMs), entailing the quantization of model parameters post the

LLM's training phase. The primary goal of PTQ is to reduce both the storage requirements and computational complexity of the LLM, without necessitating alterations to the model's architecture or embarking on a retraining process. This approach stands out for its simplicity and efficiency, particularly in achieving significant model compression. In the context of LLMs, which typically contain billions of parameters, Quantization-Aware Training (QAT) often becomes impractical due to excessive training costs. Hence, PTQ emerges as a more viable solution for these large-scale models. However, it's crucial to acknowledge that PTQ can lead to a certain degree of precision loss as a consequence of the quantization process. Despite this, PTQ serves as an effective method to enhance the efficiency of LLMs, offering a straightforward solution that avoids major modifications or extensive additional training.

In PTQ, various approaches focus on weight-only quantization to enhance efficiency. For instance, LUT-GEMM [Park et al., 2023] optimizes matrix multiplications in LLMs using weight-only quantization and the BCQ format, thereby reducing latency and improving computational efficiency. LLM.int8() [Dettmers et al., 2022] employs 8-bit quantization, which halves GPU memory usage during inference and maintains precision through vector-wise quantization and mixed-precision decomposition. This method enables efficient inference in models up to 175 billion parameters. ZeroQuant [Yao et al., 2022] combines a hardware-friendly quantization scheme with layer-by-layer knowledge distillation, optimizing both weights and activations to INT8 with minimal accuracy loss. Addressing higher compression targets, GPTQ [Frantar et al., 2022] introduces a layer-wise quantization technique based on approximate second-order information, achieving a reduction to 3-4 bits per weight with minimal accuracy loss. Additionally, the study by Dettmers and Zettlemoyer [2023] explores the balance between model size and bit precision, particularly for zero-shot performance, finding that 4-bit precision generally offers the optimal balance. Innovations like AWQ [Kim et al., 2023c, Lin et al., 2023] highlight that protecting a small percentage of salient weights can significantly reduce quantization error. AWQ uses an activation-aware approach, focusing on weight channels with larger activation magnitudes, and incorporates per-channel scaling for optimal quantization. OWQ [Lee et al., 2023] analyzes how activation outliers amplify quantization error, introducing a mixed-precision scheme to assign higher precision to weights affected by these outliers. SpQR [Dettmers et al., 2023b] takes a unique approach by isolating outlier weights for storage in higher precision, while compressing the remainder to 3-4 bits. This technique allows for more efficient compression while maintaining near-lossless performance.

To achieve even lower-bit quantization (e.g., below 2-bit), QuIP [Chee et al., 2023] introduces an innovative approach that accounts for the even distribution of weight magnitudes and the significance of accurately rounding directions unaligned with coordinate axes. QuIP comprises an adaptive rounding procedure that minimizes a quadratic proxy objective, essential for optimizing the quantization process. Additionally, it employs efficient pre- and post-processing techniques that ensure weight and Hessian incoherence through multiplication by random orthogonal matrices, crucial for maintaining quantization effectiveness. Further advancing PTQ methods, Li et al. [2023a] are inspired by the observation that aligning the quantized activation distribution with its floating-point counterpart can restore accuracy in LLMs. Their proposed 'Norm Tweaking' strategy involves a meticulous calibration data generation process and a channel-wise distance constraint. This approach updates the weights of normalization layers, leading to enhanced generalization capabilities. [Shang et al., 2023] propose partial-binarized LLM (PB-LLM) by introducing binarization [Hubara et al., 2016] into LLM quantization to push weight quantization under 2 bits. Following PB-LLM, BiLLM [Huang et al., 2024] pushes weight quantization to almost 1 bit.

Apart from efforts that focus solely on weight quantization in LLMs, numerous PTQ approaches attempt to *quantize both weights and activations*. SmoothQuant [Xiao et al., 2023a] addresses the challenge of quantizing activations, which can be complex due to the presence of outliers. It introduces a per-channel scaling transformation that effectively smooths out activation magnitudes, rendering the model more receptive to quantization. Recognizing the intricacies of quantizing activations in LLMs, RPTQ [Yuan et al., 2023a] highlights the uneven ranges across channels and the prevalence of outliers. RPTQ's innovative approach involves clustering channels for quantization, thereby reducing discrepancies in channel ranges. This method smartly integrates channel reordering into layer normalization and linear layer weights to minimize overhead. OliVe [Guo et al., 2023a] adopts an outlier-victim pair (OVP) quantization strategy, focusing on local handling of outliers with low hardware overhead and significant performance benefits. This approach stems from the understanding that outliers are crucial, while adjacent normal values are less so. Building on this, Outlier Suppression+ extends the concept by addressing asymmetrically distributed harmful outliers in specific channels. It introduces channel-wise shifting and scaling operations to balance the outlier distribution and reduce the impact of problematic channels, considering both the nature of the outliers and the subsequent quantization errors. ZeroQuant-FP [Wu et al., 2023c] delves into floating-point (FP) quantization, specifically exploring FP8 and FP4 formats. This study finds that FP8 activation quantization in LLMs outperforms the traditional INT8 format, while FP4 weight quantization shows compa-

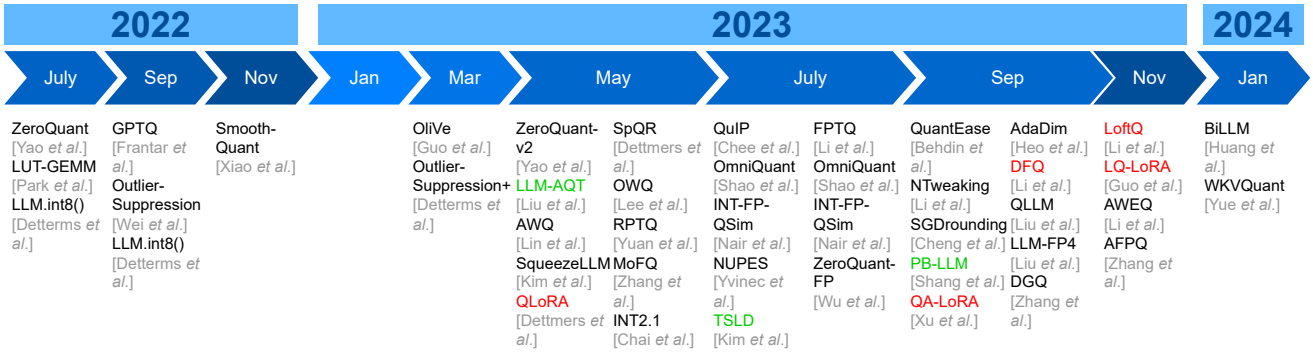

Figure 9. Timeline of Quantization for LLM methods from 2022 to 2024. The red-highlighted methods represent they belonging to Quantization for Parameter Efficient Fine-Tuning (Q-PEFT), the green-highlighted methods represent they belonging to QAT-related methods, and others are PTQ-based methods.

rable efficacy to INT4. ZeroQuant-FP addresses the divergence between weights and activations by standardizing all scaling factors as powers of 2 and restricting them within a single compute group, ensuring consistency and efficiency in the quantization process. Li et al. [2023c] propose FPTQ, in which they employ a layerwise strategy to cope with different levels of quantization difficulty. Particularly, they devises an offline logarithmic activation equalization to render a quantization-friendly distribution for previously intractable layers. [Yue et al., 2024] identifies the huge cost from key/value (KV) cache, and propose WKVQuant for quantizing weights and the KV cache of LLMs.

3.1.3 Quantization for Parameter Efficient Fine-Tuning (Q-PEFT)

Parameter Efficient Fine-Tuning (PEFT) is an important topic for LLMs. One of the most popular approaches is low-rank adaptation (LoRA) [Hu et al., 2021, Valipour et al., 2022], where the key insight is to decompose the adapter weights into the multiplication of two low-rank (and thus parameter-efficient) matrices. LoRA has claimed comparable performance to full fine-tuning while using much fewer learnable parameters. Please refer to the review paper [Hu et al., 2023] for more details about this adaptor.

In addition to the well-defined quantization paradigms, a novel paradigm in LLM efficiency is emerging: Quantization for Parameter-Efficient Fine-Tuning (Q-PEFT). This approach integrates quantization into the fine-tuning process of LLMs, offering a unique and efficient method, particularly relevant in the era of large models. Pioneering works in this paradigm, such as PEQA [Kim et al., 2023a], DFT [Li et al., 2023e], and QLORA [Dettmers et al., 2023a] demonstrate the feasibility and effectiveness of this approach. PEQA employs a dual-stage process where the first stage involves quantizing the parameter matrix of each fully connected layer into a matrix of low-bit integers coupled with a scalar vector. The second stage focuses on fine-tuning the scalar vector for specific downstream tasks, allowing for more efficient task-specific adjustments. DFT adopts the efficient Lion optimizer, which only keeps track of the momentum and has consistent update magnitudes for each parameter, an inherent advantage for robust quantization; and (ii) we quantize all model states and store them as integer values, and present a gradient flow and parameter update scheme for the quantized weights. On the other hand, QLORA introduces novel concepts such as a new data type, double quantization, and paged optimizers. These innovations aim to conserve memory efficiently while maintaining LLM fine-tuning performance. Notably, QLORA facilitates large model fine-tuning on a single GPU, achieving state-of-the-art results on the Vicuna benchmark, a testament to its effectiveness in balancing memory efficiency and model performance.

However, a limitation of QLoRA is its restriction to at most 4-bit quantization during fine-tuning; lower-bit quantization, such as 2-bit, can significantly deteriorate the performance. Addressing this challenge, several studies have ventured into the realm of Q-PEFT to enable lower-bit quantization. LQ-LoRA [Guo et al., 2023b] introduces an iterative algorithm that decomposes each pretrained matrix into a high-precision, low-rank component and a memory-efficient quantized component. During fine-tuning, only the low-rank component is updated, keeping the quantized component fixed. This method presents an integer linear programming approach for the quantization component, allowing dynamic configuration of quantization parameters like bit-width and block size within a given memory budget. Another notable approach, Loft-Q [Li et al., 2023d], simultaneously quantizes an LLM and establishes a suitable low-rank initialization for LoRA fine-tuning. This strategy effectively bridges the gap between the quantized and full-precision models, significantly enhancing generalization in downstream tasks. QA-LoRA [Xu et al., 2023c] leverages the benefits of quantizing the LLM's weights into low-bit

integers, facilitating an efficient fine-tuning stage. Additionally, it produces a lightweight, fine-tuned model, circumventing the accuracy loss often associated with PTQ.

3.1.4 Discussion on LLM Quantiztaion

Figure 9 presents a timeline of LLM quantization techniques, highlighting the evolution from Post-Training Quantization (PTQ) as the initial mainstream approach to the rising prominence of Quantization-Aware Training (QAT) and Quantization for Parameter-Efficient Fine-Tuning (Q-PEFT). This shift underscores the community's adaptation in response to the performance bottlenecks encountered with PTQ, marking QAT and Q-PEFT as the burgeoning areas of focus in the quest for efficient LLM inference.

3.2. Pruning

Pruning [LeCun et al., 1989, Liang et al., 2021], which concentrates on identifying and eliminating model parameters that are deemed unnecessary or redundant, is another popular technique for compressing LLMs. In the context of LLMs, the parameters often account for a considerable portion of the model size and computational demand. By carefully pruning these parameters, it's possible to streamline the model, making it more efficient without significantly compromising its performance. Pruning methods can be broadly classified into two categories: unstructured pruning and structured pruning, and we describe the research progress of each category in turn below.

3.2.1 Unstructured pruning

Unstructured pruning selectively eliminates individual weights or neurons from a model, leading to a sparser, yet more irregularly structured network. This form of pruning excels in ensuring model accuracy, however, the resultant irregularity in the weight distribution necessitates specialized handling or software optimizations. SparseGPT [Frantar and Alistarh, 2023] is a groundbreaking one-shot pruning method tailored for LLMs. It tackles the pruning challenge by reconceptualizing it into a series of extensive sparse regression problems, efficiently solved by a newly developed solver. Notably, SparseGPT can efficiently process a model with 175 billion parameters in just a few hours on a single GPU, and it can induce significant sparsity (50-60%) in LLMs without significantly sacrificing accuracy or necessitating fine-tuning. To tackle the challenge of reconstruction cost in SparseGPT, Sun et al. [2023a] propose Wanda, which assesses the significance of each weight by evaluating its magnitude and the norm of the corresponding input, significantly increasing the computational efficiency. Further, Yin et al. [2023] design a set of non-uniform hierarchical sparsity ratios to pay more attention to the layers with higher outlier occurrences, thus boosting the pruning performance. Moreover, Considering the hardware support for unstructured pruning, Flash-LLM [Xia et al., 2023a] proposes an unstructured sparse matrix multiplication method, which is characterized by sparse loading and dense computation, to implement the GPU Tensor Core's sophisticated support for unstructured sparsity.

3.2.2 Structured pruning

Structured pruning removes entire neurons or layers, resulting in a cleaner, more regular structure. The pruned model is generally more compatible with conventional hardware, however, the simplicity and regularity come at a cost: this form of pruning can have a more pronounced impact on the model's performance, as it involves removing larger, potentially more critical components. LLM-Pruner [Ma et al., 2023] represents a pioneering approach in structural pruning for LLMs. It employs a one-shot pruning technique, which relies on first-order and estimated Hessian data and necessitates subsequent fine-tuning using LoRA to restore the weights. This work is advantageous as it significantly reduces both computational demands and memory requirements, while preserving the fundamental structure of LLMs. Sheared LLaMA [Xia et al., 2023b] proposes another noteworthy solution by combining targeted structured pruning with a dynamic batch loading algorithm. First, it meticulously prunes a source model into a desired target architecture, meticulously chosen by analyzing the configurations of the pre-trained model. Then, it enhances training efficiency through the dynamic batch loading algorithm, which adjusts the proportion of training data from various domains. Compresso [Guo et al., 2023c] establishes a collaborative learning framework, where the LLM and a resource-efficient pruning algorithm work in tandem, with the ability to prune LLaMA-7B to 5.4B while preserving the original performance.

3.3. Knowledge Distillation

Knowledge distillation [Gou et al., 2021, Hinton et al., 2015] is a technique that facilitates the transfer of capabilities from a larger model (referred to as the "teacher") to a smaller model (referred to as the "student"), allowing the smaller model to perform tasks with similar proficiency as the larger model but with reduced computational resources [Gou et al., 2021, Shang et al., 2021]. For LLM compression, there are two main categories of knowledge distillation: white-box and black-box distillation. Within these categories, researchers have developed a range of distillation methods tailored for LLMs, which are described in detail below. Moreover, a more detailed and specific survey regarding Knowledge Distillation of LLMs has also been carried out [Xu et al., 2024].

3.3.1 White-Box Knowledge Distillation

In white-box distillation, the internal workings and architecture of the teacher model are fully accessible and utilized during the distillation process. This transparency allows the student model to learn not just the output of the teacher model but also its internal representations and decision-making processes. MiniLLM [Gu et al., 2023] critiques the limitations of standard knowledge distillation objectives and suggests that reverse Kullback-Leibler divergence is more effective for capturing the complexity of generative tasks, which can enhance the student model's response quality and reliability. MiniLLM also introduces single-step regularization, teacher-mixed sampling, and length normalization to address challenges in training, thus demonstrating great performance potential for distilling LLMs on the standard benchmarks. In contrast to MiniLLM, GKD [Agarwal et al., 2023] presents a more straightforward and stable method. It aligns more with supervised training by avoiding backpropagation through the student model's sampling. Instead of using predetermined output sequences, GKD trains the student model on its own created sequences, utilizing the teacher's probabilities as guidance, which leads to notable improvements in the student's performance. Homotopic distillation [Liang et al., 2023a] aims to facilitate the alignment of the student model's predictions with those of the teacher model across extensive open-domain data. It involves starting the student model with the teacher model's configuration and progressively reducing the student model's neurons to reach a specified model complexity. Furthermore, Liang et al. [2023b] present a layerwise distillation approach that involves creating unique task-aware filters for each layer of teacher and student models. These filters, essentially neural networks equipped with task-specific heads, are designed to distill and capture the predictive knowledge from the hidden layers of the respective models. AD-KD [Wu et al., 2023b] analyzes the teacher model's token-level rationale using integrated gradients and transfers attributional knowledge to the student model, which enables the student model to imitate the teacher's underlying reasoning, not just its behaviors.

3.3.2 Black-Box Knowledge Distillation

Contrary to white-box distillation, black-box distillation does not require access to the internal mechanisms of the teacher model. Instead, it focuses on replicating the output behavior of the teacher model. The student model learns solely from the input-output pairings produced by the teacher, without any insight into its internal operations. Multitask-ICT [Huang et al., 2022] introduces in-context learning distillation, which merges the objectives of in-context learning with those of language modeling, intending to distill into smaller models both the capability to comprehend in-context examples and the knowledge required for specific tasks. LaMini-LM [Wu et al., 2023a] creates a set of 2.58 million instructions and employs GPT-3.5 Turbo to produce responses to these instructions. Subsequently, it uses these instructions as a basis to fine-tune a range of student models. Similarly proceeding from creating examples, Sahu et al. [2023] proposes PromptMix, which involves a two-step method based on prompting to create labeled examples for text classification. In PromptMix, the borderline examples can enhance the knowledge transfer from teacher models like GPT-3.5 to student models. In contrast to the traditional unidirectional knowledge distillation, Lion [Jiang et al., 2023] introduces an adversarial distillation framework, which encourages the teacher model to identify "hard" instructions and subsequently generate new "hard" instructions for the student model, resulting in a dynamic three-step adversarial cycle.

Black-box distillation is also identified as a promising tool to transfer the power of chain-of-thought (CoT) prompting from larger models to smaller ones. Fu et al. [2023b] observe a trade-off in language models between their diverse capabilities, and focus on moving the teacher model's capability from general abilities towards enhancing the student model's proficiency in the targeted mathematical CoT. SCOTT [Wang et al., 2023] uses contrastive decoding for better rationale supervision and a counterfactual reasoning objective for faithful distillation, resulting in more faithful CoT rationales. Distilling step-by-step [Hsieh et al., 2023] introduces a novel training method for smaller models, surpassing LLMs with less data. It uses LLM rationales as extra training material in a multi-task framework, cutting down data needs versus standard fine-tuning and distillation. Similarly, Li et al. [2023b] propose symbolic CoT distillation, where they obtain CoT rationales for unlabeled dataset instances from the teacher model and then train the student model to forecast both the rationale and the label based on these instances. To promote complex, multi-step reasoning within a dialogue context, i.e., dialogue CoT reasoning, Chae et al. [2023] utilize LLMs as inconsistent teachers and strategically distill valuable and logical rationales through alignment filters.

3.4. Factorization

The use of low-rank matrix decomposition [Kishore Kumar and Schneider, 2017] as a technique for compressing Deep Neural Networks (DNNs) represents a straightforward yet effective approach, garnering considerable attention within both scientific computing and machine learning domains. In recent years, the challenge of efficiently compressing and accelerating large-scale neural networks via low-rank methods has become a focal point of research. This has led to significant advancements in developing and refining low-rank factorization strategies tailored for DNNs [Schotthöfer

et al., 2022].

Activation-aware Singular Value Decomposition (ASVD) [Yuan et al., 2023b] is the first work using factorization techniques to compress LLM. ASVD effectively manages activation outliers by adjusting the weight matrix based on the activation distribution, improving decomposition accuracy and efficiency. ASVD also addresses the varying sensitivity of different LLM layers to decomposition, with an iterative calibration process for optimal layer-specific decomposition. Concurrently, LAyer-SElective Rank reduction (LASER) [Sharma et al., 2023] demonstrates the surprising result that it is often possible to significantly improve the performance of LLMs by selectively removing higher-order components1 of their weight matrices. Apart from targeting the LLMs' weights, TensorGPT [Xu et al., 2023b], in which the embedding layer of LLMs is compressed through Tensor-Train Decomposition (TTD) [Oseledets, 2011] in order to store large embeddings in a low-rank tensor format, with much fewer parameters.

4. Algorithmic Methods for Fast Decoding

Large Language Models (LLM) have achieved astonishing performance in various text generation tasks such as Machine Translation, Article Summarization, and Question Answering. To complete these tasks, popular LLMs typically contain the decoder structure that generates tokens one after another, following an autoregressive relation with all preceding tokens. During the decoding of every token, decoder weights have to be repeatedly loaded into memory. Because of the autoregressive nature, the memory loading is innately sequential and cannot be easily parallelized. As the parameter size of LLM becomes colossal, the decoding process becomes heavily memory-bound (de Jong et al. [2023]) and experiences low hardware utilization, leading to severely long latency (Kim et al. [2023d]). Text generation tasks are the fundamental building block for extremely popular real-world applications such as ChatBot (OpenAI et al. [2023]) which demands swift even real-time responses. Finding ways to reduce LLM inference latency is now an urgent problem.

This section focuses on the discussion of prior efforts to reduce the LLM inference latency from an algorithm perspective. We are aware of the ample previous attempts from the system and hardware perspectives and defer the discussion of them in Sections 5 and 6. Also, model compression techniques introduced in Section 3 can directly reduce the parameter size of the LLM and decrease the inference latency, as LLM inference is memory-bound. However, these techniques inevitably lead to performance degradation to tradeoff the model size shrinkage, which is potentially unacceptable for certain real-world applications. This section looks at prior works that reduce LLM inference latency but need to store the entire LLM in the machine storage to preserve the text generation quality. Specifically, this section intends to develop the discussion from two directions:

- In section 4.1, for every single token decoded (fixed #tokens decoded), how to utilize the minimum number of parameters of the LLM.
- In section 4.1.1, for every single forward propagation of the LLM (fixed #parameters used) how to decode the maximum number of tokens.

4.1. Minimum Parameter Used Per Token Decoded

Interestingly, Simoulin and Crabbé [2021] has shown that although language models tend to have a huge number of parameters, not all parameters are needed to decode the accurate tokens. LLM inference latency can be reduced by selecting only a subset of necessary parameters to use (load) per input token and still preserving the decoded token's accuracy. In this section, we look at input-dependent dynamic weights dropping scheme for LLM from three different perspectives: 4.1.1 looks at early exiting, or dynamically choosing weights in the layer, depth, dimension; 4.1.2 introduces novel methods that dynamically detects sparsity in the width dimension of the LLM, pruning out heads and MLP columns; 4.1.3 present Mixture-of-Experts (MoE) which pretrains a sparse model and chooses the correct experts for the different input during runtime.

4.1.1 Early Exiting

Early exiting has been a well-explored idea in various network architectures, particularly for the encoder-only models. (Baier-Reinio and Sterck [2020], Hou et al. [2020], Li et al. [2021], Liu et al. [2020], Liu et al. [2022], Schwartz et al. [2020], Stickland and Murray [2019], Xin et al. [2020], Zhou et al. [2020], Zhu [2021], Schuster et al. [2021]). However, the LLMs that specialize in continuous token generation at the sequence level rely particularly on the decoder architecture. Early exiting for decoder architecture requires consistency and quality retaining on the sequence level where each token depends on the previous tokens, which are considerations lacking in the previous abundant encoder-only early-exiting literature. The decoder contains layers of identical structure. Benefiting from this trait, the output hidden states of every layer can be used to pass in the LM Head to get a probability distribution prediction of the next token decoded. Geva et al. [2022] and Simoulin and Crabbé [2021] observe that for some tokens, the hidden states saturate during the intermediate layers. In other words, early exiting in the middle would, for some tokens, output the correct top-1 prediction as running through the full model. This observation lays the basis for the success of decoder early exiting methods. Elbayad

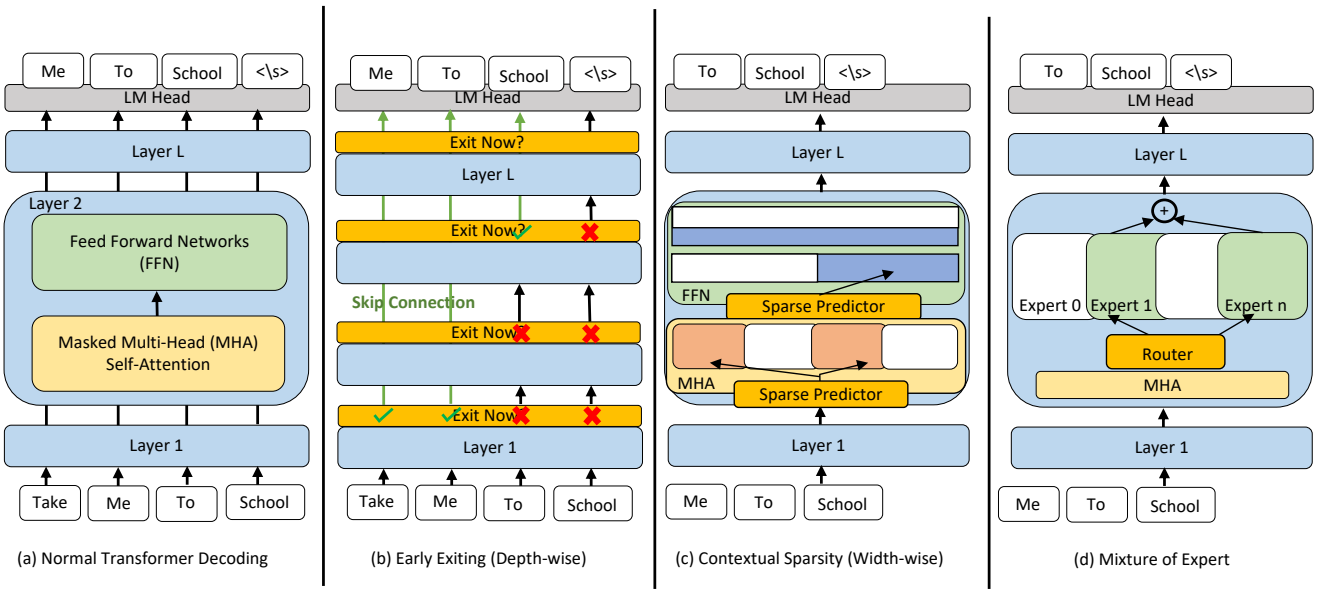

For some tokens, only a necessary subset of weights is needed to decode correctly. (a) presents the normal decoder-only autoregressive model architecture; (b) Early Exiting aims to only use the necessary transformer layers that already produce correct decoded tokens and skip the rest of the layers, but challenges arises when different tokens exit at different layer across. Same gist also applies to the width dimension of the LLM. (c) represents a line of works that predicts the dynamic sparsity on attention head and linear layers column dimension in the input-dependent way. (d) presents the Mixture of Expert method which has the sparsity built-in to the pretrained model. During inference, a router aims to choose concise and proficient expert networks that depending on the input. (Illustration best viewed with color)

Figure 10. Illustration of Input-Dependent Dynamic Network Technique

et al. [2020] conducts an early effort for efficient machine translation tasks to use early exiting on the decoder architecture. It proposes a general approach to follow. Shown in Figure 10 (b), during the forward propagation, after every layer, there is an internal confidence function, usually a fixed metric or an MLP with a small number of layers, that computes a confidence score based on the hidden states on how likely it is to saturate at the current layer. The score is used to decide whether to exit through some carefully designed criteria. The LM Head is then used to output the next token-predicted probability distribution. Due to the high similarity of the newer follow-up works, we extend the discussion by looking at the key challenges of designing early exiting schemes for language models, where they introduce different novel techniques.

Modeling the Confidence of Saturation CALM Schuster et al. [2022] studies three different ways to output the confidence score to exit: the softmax response, or the difference between the top two values after the softmax; the saturation of hidden states, or the cosine similarity between the current layer's hidden states with the last layer; the output of a linear classifier inserted to every layer. The linear classifier is trained by simply using a cross-entropy loss to align MLP output when inputting the hidden states with whether the top-1 token decoded as exiting on the current layer matches the top-1 token decoded of the full model. The experiments presented suggest that despite not being the most accurate predictor, the classifier method reaches the optimal trade-off between additional FLOPs overhead with prediction accuracy on score generating. Building up from CALM, Bae et al. [2023] observed that when consistently exiting from shallow layers will result in an abnormally long length. Also, the confidence score computation on every layer injects high overhead and diminishes the benefit of early exiting. Therefore, it proposes to only have two choices for early exiting: either exit from the so-called "shallow module" or a group of shallow layers, or go all the way to the full model, or "deep module", drastically reducing the number of classifiers needed inside the model. Such design enables it to achieve more speedup than CALM, reaching 2x for certain tasks. On the other hand, ConsistentEE Zeng et al. [2023] proposes a different method to predict when to exit. It uses an RL policy network that is iteratively trained with the per-layer output classifier head. The policy networks are trained with the goal of balancing the optimization of both efficiency (the early layer receives rewards) and accuracy (the reward function has a term that is the early exit output CE loss).

Early Exit Criteria CALM Schuster et al. [2022] proposes

a distribution-free calibration technique that uses the fixed sequence testing procedure (Family-wise Error Rate procedure) to output the suitable threshold. The threshold is exponentially decreasing to allow more aggressive exiting for tokens later in the sequence. Bae et al. [2023], on the other hand, observes that the pattern of confidence criteria resembles a beta distribution and uses the on-the-fly data to update a beta distribution model through MLE and use such probability model to guide its decision. Zeng et al. [2023] bypasses this issue by letting the policy network directly output the exit decision.

Hidden States Propagation Hidden states of the skipped layers can pose a technical challenge. As shown in the 10 (b), the token position at "school" exits later than previous tokens. However, the last self-attention layer doesn't have the previous key-value pairs of the previous early exited tokens. Elbayad et al. [2020] and Schuster et al. [2022] proposes the "hidden states propagation" technique. For example, the hidden states of token "Max" at the exited layer l_1 are stored. When the later token "school" reaches deeper layer l_2, the hidden state for "Max" is copied for all layers between l_1 and l_2, and the key-value pairs are then computed on the copied hidden states. Basically, to approximate the deep layer's hidden state with the ones from the early layer. Later works Bae et al. [2023] and Ding et al. [2023] found that state propagation leads to performance degradation. Since LLM inferences are dominated mostly by memory loading, computation is relatively "free". These two methods proposed to recompute the later hidden states directly on the fly. Chen et al. [2023b] proposes to run the full large model in parallel to the early exit stream to efficiently parallel the computation of the missing kv cache. Din et al. [2023] conducts a systematic study on using a linear network to jump across layers for transformer architecture and shows that linear layers can be added to effectively bridge the performance gap between directly copying and computing the hidden states with low memory and compute cost. SkipDecode Corro et al. [2023] chooses an aggressive approach to prioritize the speedup and relax the performance preservation goal. By utilizing the observation that a token coming later in the same sequence on average requires less number of layers to decode the correct tokens, it completely bypasses the need for state propagation by forcing the maximum layer used to be monotonically decreasing for deeper positions. Besides, SkipDecode also introduces fixed exit points to optimize for batched early exit.

Output Classifier Training When exiting from intermediate layers, the intermediate hidden states need to go through an output classifier head to output prediction of the next token probability distribution. The output classifier can either be shared as shown in Figure 10 or per-layer independent. These classifiers are usually trained to better adapt to the early exiting pattern. Elbayad et al. [2020] proposed to have an average CE loss of all layers to be the training loss of the classifier. On the other hand, Schuster et al. [2022] uses a weighted average where weights increase as the layer number increases, assigning more contribution to deeper layers. Bae et al. [2023] introduces a dynamic knowledge distillation loss which dynamically assigns the "shallow module" a suitable hidden state from the "deep module". Both Rotem et al. [2023] and Ji et al. [2023] find a "conflicting gradient" issue when joint training with the same loss across all models: Rotem et al. [2023] detects the gradient conflict between early and later layers of language models, while Ji et al. [2023] spots the "orthogonal gradient" between the objective to improve semantic awareness and the objective to improve early exciting decision. Both methods propose adding an additional block of parameters and iterative training to alleviate the issue.
Besides the above-mentioned perspectives, Chen et al. [2023b] studies system-level optimization techniques to efficiently run LLM early exit under the 3D parallelism setting.

4.1.2 Contextual Sparsity

While early exiting aims to select parameters on the depth dimension, some techniques have also been proposed to exploit the dynamic sparsity on the width dimension. Deja Vu Liu et al. [2023c] conducts a comprehensive study on dynamic sparsity on the LLM width dimension. The paper reveals that contextual sparsity can go up as high as 80%, meaning that the majority of the weights can be left out while still preserving the original model performance. However, the chosen weights are dynamic and different for different input tokens. The paper formulates this problem as a nearly neighbor search problem that for a given hidden state from the embedding layer of previous layers, how to find the attention heads and the MLP columns that are the most similar to these tokens. To save compute, the paper proposes to train a small MLP network as the Sparse Predictor in front of the Multi-Head Attention (MHA) and the Feed-Forward Networks (FFN) of the LLM, shown in Figure 10 (c). By using only a subset of weights and reducing the memory IO overhead, Deja Vu manages to achieve over 2x speedup of LLM inference. Building on Deja Vu, PowerInfer (Song et al. [2023]) brings the contextual sparsity finding to the LLM inference across heterogeneous devices (CPUs and GPUs). PowerInfer discovers a substantial portion of weights are heavily used and activated in the input-independent setting, thus stored on the GPU memory, while others are on the CPU memory. Then, to specifically find the weights to use for a given input token, it trains

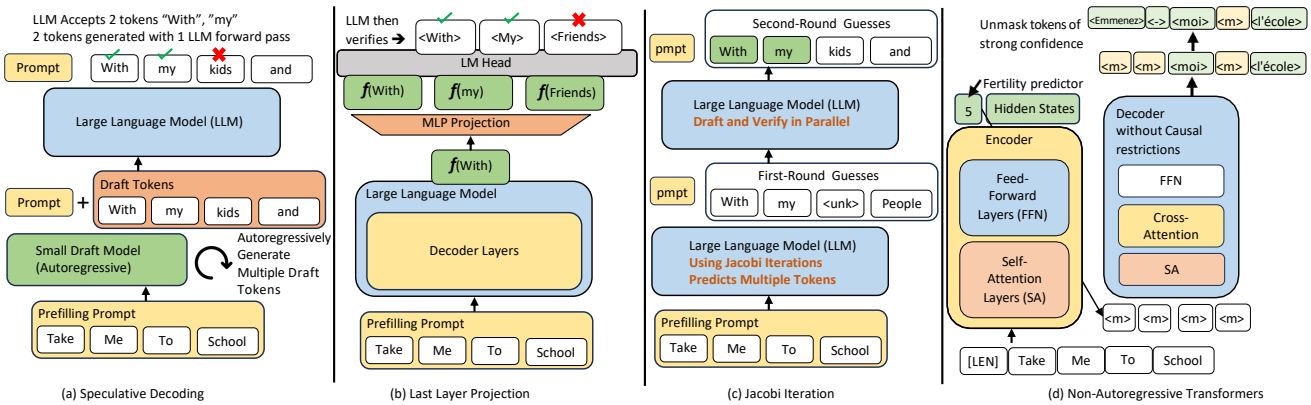

Several methods have been proposed to generate more than one token per LLM forward prop: (a) shows the speculative decoding which asks the LLM to, instead of generate tokens autoregressively, evaluate tokens generated by the small model all at once to parallelize the memory loading; (b) introduces another approach to have a last layer projection on the large model hidden state vector to generate tokens at subsequent positions; (c) presents another method to treat decoding as solving a system of nonlinear equations and use Jacobi and Gaussian-Seidel iteration algorithm to parallelize the decoding process of a number of token positions; (d) presents the Non-Autoregressive Transformers which targets the seq-to-seq model. The decoder relaxes the autoregressive constraints and iteratively decode all the tokens from masked tokens based on the information from the encoder model hidden states.

Figure 11. Illustration of the Parallel Decoding Methods

a smaller sparse prediction than Deja Vu. To make the sparse predictor, it initializes the sparse predictor to have a dynamic structure and iteratively trains and modifies the sparse predictor. To better do inference of the model deployed on the mixed CPU and GPU environment, it introduces a novel memory placement scheme and implements a vector-based sparse computation library. Concurrently, MatFormer (Devvrit et al. [2023]) studies the problem of LLM deployment on various heterogenous devices of different hardware capabilities. They added dynamic structure only on the FFN, which occupies 60% of total weights. The model is specially trained so that during inference, based on the target hardware properties, MLP layers are sampled on the row dimension to give a model of various sizes with reasonable performance. To diversify the model size selection, it imposes a Mix'n'Match method to choose different settings for different layers, so combined would give a more variable model size.

4.1.3 Mixture-of-Expert Models

Language Models, especially transformer architecture, exhibit strong power-law scaling (Kaplan et al. [2020], Hoffmann et al. [2022]) of performance when the training dataset is scaled up. On the other hand, though bringing strong performance gain, the large parameter count makes training and inference of the model inefficient. The mixture of expert (MoE) technique is a well-studied topic (Yuksel et al. [2012]) that effectively decouples the parameter count of the model and the computation FLOPs required by the model training and inference, thus bringing huge gains of efficiency under certain conditions. Further, MoE is shown to effectively scale up the language model size and increase its performance without the concern of increasing compute during inference (Lepikhin et al. [2020], Fedus et al. [2021]). Shown in Figure 10 (d), an expert network is inserted into the transformer architecture to replace the FFN layers. Also, a gating function is introduced between the Multi-Head Attention and the expert network which aims to select the best-fit expert or experts for the given input token. For in-depth analysis and discussion about the MoE scaling generalization, routing algorithms, training techniques, etc., we refer the readers to the survey on Sparse Expert Models (Fedus et al. [2022]). *Although both rely on the input token to determine sparse structure, We deliberately separate MoE and the contextual sparsity techniques because the latter operates on pre-trained dense language models and exploits the sparsity from the dense neural networks, while the prior trains a sparse model from the beginning.* More recently, MoE techniques have achieved substantial success. Sparse Mixer (Lee-Thorp and Ainslie [2022]) brings 89% and 98% speedup in both training and inference to BERT (Devlin et al. [2019]) models. Du et al. [2022] uses only 49% FLOPs but beats GPT-3 (Brown et al. [2020]) in performance. ST-MoE (Zoph et al. [2022]) brings MoE to the encoder-decoder models, even becoming the state-of-the-art model for many reasoning and generation tasks. ST-MoE, using 20x and 40x fewer FLOPs in training and inference, beats 540B PaLM (Chowdhery et al. [2022]) in performance. Mixtral 8x7B (Jiang et al. [2024]), while only actively using 13B parameters during inference, performs on par with Llama2-70B models (Touvron et al. [2023b]) across various evaluation benchmarks.

Besides, various attempts have been made to optimize MoE model inference. Kossmann et al. [2022] builds an efficient compiler library RECOMPILE for MoE models that introduce dynamic recompiling and optimization according to varying inference batch sizes. Rajbhandari et al. [2022] extends the ZeRO distributed inference method to MoE models. Jawahar et al. [2023] conducts Neural Architecture Search (NAS) on the expert network architecture. Yi et al. [2023] deploys large MoE language models on the edge devices. It optimizes the deployment around the finding that some neurons are much more heavily used in the MoE models than others.

4.2. Maximum Tokens Decoded Per LLM Forward Propagation

Another angle to reduce the latency of LLM inference is to relax the LLM from the limitation of autoregressive decoding and have more than one token decoded per one LLM forward propagation. We look at two ways to achieve it: 4.2.1 presents the speculative decoding method which introduces a computationally efficient draft model to propose candidates for the next few token positions, while the LLM is used to evaluate the draft model's proposed draft tokens, instead of generating next tokens. On the other hand, 4.2.2 presents works that enable the LLM to directly decode multiple tokens from a single forward propagation. Due to some methods combining the benefits from both directions and lying in the middle, we manually add a distinction just for the sense of nomenclature that speculative decoding methods here all have the draft model to be in the transformer architecture.

4.2.1 Speculative Decoding

Due to the demanding memory loading challenges and autoregressive properties, LLMs are inefficient in inference. However, models that are much smaller in size are shown (Kim et al. [2023e]) to have the ability to decode the correct sequences as the LLM, as long as some key tokens in the sequence of the small model generation are corrected. Then, shown in Figure 11 (a), when the small model is asked to infer (speculate) and output a sequence of draft tokens, memory loading of model weights is less of a problem, resulting in much higher utilization in hardware computation units. To ensure the quality of the text generated by the small model, the LLM can "periodically" evaluate and correct tokens from the small model's draft. Then, although the large model needs to sometimes evaluate the wrong draft tokens, potentially leading to larger FLOPs spent than LLM autoregressive decoding, the memory loading of weights is parallelized on the token dimension and drastically reduces the memory IO overhead. Since the LLM inference is memory bottlenecked, the speculative decoding will potentially reduce the LLM inference latency greatly.

LLM Distribution Preserving During early exploration of this idea, two different paths emerged concurrently. Kim et al. [2023e] proposed to have the small model speculate and generate draft tokens until the token decoded confidence falls below a threshold. Then, the small model "fallback" to the large model to evaluate the draft tokens generated and hand over to the small model. Some of the tokens are rejected, so the large model asks the small model to "roll back" these wrong tokens and resume speculating. In the paper's setting, all decoding is "greedy". The paper show that the large and small model pair can generate text with quality on par with the original large model autoregressive generated text. However, Leviathan et al. [2023] and Chen et al. [2023a], upon the small model speculate paradigm, points out a technique of resampling that at the position where the LLM rejects the small model's prediction that provably enables the large and the small model predictions to be in the same probability distribution as the large model's autoregressive generation. The following techniques generally follow the paradigm of speculating then evaluating and resampling to preserve the LLM autoregressive decoding quality while enabling speedup.

Building a Tree of Draft Tokens Since the LLM generates in the autoregressive order, every token is dependent on all previous tokens generated, and the length of the accepted tokens in the small model's draft is usually modest and bounded. It is exponentially more difficult to speculate on tokens more distant in the future. For example, if the small model is asked to output the length m draft sequence, and the LLM accepts n, $n < m$, the (m - n) tokens are automatically discarded. Thus, the speedup ratio of speculative decoding is modest, since every LLM forward leads to only a limited number of tokens being decoded. There are two ways to improve the speedup of speculative decoding. First, Sun et al. [2023b], Miao et al. [2023b], and Xu et al. [2023a] all proposed to boost the draft on the batch size direction, or letting the small model sample multiple plausible draft sequences for the LLM to evaluate in parallel. Specifically, Sun et al. [2023b] proposes a way and theoretical guarantees for the LLMs to batch verify and resample from the multiple small model drafts so that the LLM distribution is preserved and no loss of generation quality is incurred. The paper first connects speculative decoding to the broader problem of discrete optimal transport. The small model is asked to sample multiple draft sequences using topk sampling. Based on

the properties of the discrete optimal transport, finding the optimal method to evaluate and resample becomes finding the optimal transport path. On the other hand, besides from maintaining the speculative decoding consistency of draft trees, Miao et al. [2023b] constructs the token tree not based on the top predictions from the small draft model, but based on multiple diversely trained small draft models, each running in parallel and output diverse but powerful draft sequences. The paper proposes a novel draft token tree construction algorithm that builds a tree of candidate tokens based on the diverse draft sequences through predefined expanding and merging schemes. Then, the large model is asked to parallel verify the constructed tree using a carefully designed tree attention to maximize the reuse of the key-value cache and maintain a tree-based causal mask. Xu et al. [2023a] innovatively applies the benefit of speculative decoding to edge devices. The paper builds an LLM serving engine for the edge, where a smaller draft LLM is sitting consistently in memory, while a larger robust LLM is occasionally loaded in memory to do verification. To boost the acceptance rate from the large LLM, it also constructs a tree using topk tokens. To cater to the edge hardware characteristics, it implements a tree-based parallel verification decoder equipped with masking and a customized large-small LLM computation pipeline to avoid memory contention.

Knowledge Distillation and Self-Speculative Decoding Another way to improve the acceptance rate is to improve the small draft model's ability to align with the LLM's generation distribution, which can be done through finetuning the small models on corpus generated by the large models with knowledge distillation. Zhou et al. [2023] establishes a mathematical connection between the acceptance rate and natural divergence between the small model and the LLM: minimizing the divergence is maximizing the acceptance rate. The paper also studies a range of different knowledge distillation losses and shows that adding knowledge distillation brings consistent 10-45% improvement in latency speedup. However, the paper generally finds that the optimal knowledge distillation loss choices vary model by model and should be tuned as a hyperparameter. Liu et al. [2023a] also shows that knowledge distillation boosts the small model training. Besides, the paper brings speculative decoding to the cloud online learning settings. LLM inference is memory-bottlenecked, which means that there is always a surplus in computation resources. The compute can be used to train a draft model continously on server, which brings two benefits: Continuously training with knowledge distillation boosts its acceptance rate and, thus, reduces the LLM inference latency; 2) serving input is constantly shifting in domains, and continuous training helps the draft models maintain the strong performance in different domains. Zhang et al. [2023] avoids storing a separate draft model by selectively sampling a smaller draft model from the large model itself. Before deployment, the paper utilizes a Bayesian optimization method to search for a draft model by skipping intermediate layers within the pretrained large model. Besides, it proposes an adaptive threshold selection technique tailored for the decoding of the draft model sampled from the large models.

4.2.2 Parallel Decoding

Alternatively, abundant works have been proposed to enable the large model to directly perform parallel decoding without the help of a small transformer model.

Simultaneously Predicting Multiple Future Tokens A wide variety of works are exploring the subject of enabling multiple token predictions directly from one forward pass of the Large Language Model. Stern et al. [2018] pioneers the design of inserting a linear projecting layer between the last hidden states output and the input of the language modeling head to enable multiple future tokens to be projected solely based on the current token's last hidden states as input. Evaluation is subsequently made by the LLM to decide whether to accept or reject these projected tokens. The proposed technique focuses on the sequence-to-sequence models that have the decoder structure. More recently, Cai et al. [2024] extends the previous work to the decoder-only language models as shown in Figure 11 (b). Besides the last layer projection, to further improve the decoded acceptance rate, the paper proposes to add a tree-based decoding structure and the associate attention mask design to propose multiple drafts simultaneously for the large model to evaluate. Besides, concurrently Monea et al. [2023] proposes to add several dummy tokens at the end of the input sequence are called "lookahead embeddings" in work. During the forward pass of each layer, the information of previous prompt tokens and already decoded tokens can be used to parallel decode several consecutive future tokens. To enable this design, the work trains a separate embedding layer that specifically serves these lookahead embeddings. Li et al. [2024] also aims to do parallel decoding with LLM evaluation. Like previous works, it also adds a lightweight structure FeatExtrapolator. Differently, the structure takes both the previous token's last layer hidden states and the actual decoded token embedding as input and output the hidden states prediction of the next layer. The LM head of the LLM is used, and several tokens are sampled, which are then used to build a decoding tree for the LLM to evaluate in parallel.

Retrieval of Frequent N-grams Besides directly using

the LLM to output several following tokens, some works use the frequently appeared n-grams in natural language to enable multiple future tokens to be generated within one forward pass of the large model. LLMA (Yang et al. [2023]) first observes that the generation tasks tend to ask the LLM to repeat tokens that appeared in the previous contexts. Based on this information, the paper set out to use the decoded tokens and the prompt to do prefix matching with a set of reference documents so that if a repetition occurs, tokens that are repeated can be directly copied to the current place. Then, an LLM will evaluate these found candidate tokens from the previous context to decide whether to use them. He et al. [2023] further extends LLMA and proposes to first construct a database of common phrases based on the LLM pretrained or finetuned dataset and corpus. Then, during decoding, the previous context prompts or tokens are used as the query to be used to retrieve into the constructed database. The candidates retrieved are organized into a prefix tree structure or a trie, which the LLM can then evaluate efficiently. Lan et al. [2023] similarly follows to use the retrieval methods to speed up inference. In contrast, it adds an extra attention layer at the end of the LLM to use the current context represented by the hidden states of the current token as the query to attend to relevant phrases retrieved from the documents of reference and select top phrases based on the attention scores.

Hierarchical Structure In Language Hierarchical Structure exists in language. For writing a long piece of article, the usual approach is to first write out the general outline of the paper, as in the format of bulletin points. Then, for every bulletin point, arguments can be extended to encapsulate the full intent of the bulletin point. Based on the observation that arguments for different bulletin points are relatively independent in semantics, some methods are proposed to parallelize the generation process for different bulletin points. Skeleton-of-Thoughts (Ning et al. [2023]) proposed to first ask the LLM to generate concise bulletin points for an article, and then collect these bulletin points on the batch axis and feed them into the LLM again as a prompt to ask the LLM to expand the arguments for each bulletin points in parallel. The achieved speedup is approximately 2x, but with the caveat that the method cannot easily generalize to all text generation tasks. More recently, APAR (Liu et al. [2024]) extends upon this direction. The paper adds specific soft tokens that explicitly inform the LLM of the hierarchical information during the generation. The LLM is further instruct-tuned to incorporate the added special tokens, and the generation is boosted with the Medusa (Cai et al. [2024]) technique to achieve 4x speedup on text generation with the hierarchical structure.

Jacobi and Gaussian-Seidel Iterative Algorithms Song et al. [2021] pioneers the study of using parallelizable methods to approximate the results from iterative and sequential inferences of fully connected networks or CNNs. Though seemingly in-viable, the paper finds that neural networks can tolerate numerical approximation errors and the data patterns that neural networks learn expose parallel structures to some extent, which makes it possible in some scenarios to parallelize the sequential inference of neural networks. Jacobi and Gaussian-Seidel Algorithms were previously proposed to solve a system of non-linear equations (Ortega and Rheinboldt [2000]) and are shown to effectively parallelize the sequential neural network inference. Santilli et al. [2023] extends the Jacobi and Gaussian-Seidel algorithms to parallelize the autoregressive decoding in the Machine Translation tasks. Specifically, this work is built on top of the previous Non-Autoregressive Transformers architecture (which we will cover later in the chapter) to enhance the parallel decoding with GS-Jacobi algorithms. The parallel decoding process stops when a [EOS] token is found in the decoded text. Concurrently, Lookahead decoding (Fu et al. [2023a]) shown in Figure 11 (c) extends this method to parallelize the LLM generation of subsequent tokens. Besides using the vanilla Jacobi iterative algorithm, it also boosts its speed with a retrieval-based algorithm to reuse the previously seen n-grams. In addition, it parallelizes the lookahead step and LLM verification step by introducing a carefully designed attention mask to the original LLM model to further improve decoding efficiency.

Non-Autoregressive Transformers For Machine Translation tasks that require autoregressive decoding of the sequence-to-sequence model, Non-Autoregressive Transformers (NAT) has been proposed to iteratively decode all of the output tokens together, as shown in Figure 11 (d). NAT has been relatively well-explored (Gu et al. [2017], Wang et al. [2019], Li et al. [2019], Sun et al. [2019], Wei et al. [2019], Shao et al. [2020], Lee et al. [2018], Ghazvininejad et al. [2019], Guo et al. [2020], Gu and Kong [2020], Savinov et al. [2021]), and we point the readers to the following survey paper that covers specifically NAT models Xiao et al. [2023b] for an in-depth review and analysis on the subject. Coarsely, the speedup of text decoding comes from making a single forward pass of the decoder output more than one token. The input sequence is first fed into the encoder, which outputs the hidden states that extract the input semantics. The output hidden states of the encoder are then used as the condition for the decoder pass. To speed up the text generation, the decoder side relaxes the autoregressive constraints and takes a sequence full of dummy tokens [pad] as the input to start the iterative parallel decoding process. During each iteration, based on the condition set by the encoder output hidden states, some tokens can be

confidently predicted, which are unmasked. The sequence is mixed with unmasked decoded tokens and the remaining masked tokens are fed to the decoder again until every token is decoded. The length of the sequence fed into the decoder, or fertility, is usually learned either inside the encoder as a special [CLS] token or by a specialized fertility predictor between the encoder and the decoder. More recently, Savinov et al. [2021] treats the decoder as a diffusion model and trains it to denoise the noisy initial sequence based on the conditions given. However, because of the requirement to use encoder hidden states as the condition for parallel decoding, NAT methods face natural difficulties in extending directly to decoder-only architectures.

5. System Optimization

To-be-updated in the 2nd version.

6. Hardware Optimization

To-be-updated in the 2nd version.

7. Conclusion

In this work, we review on efficient large language model (LLM) inference. For this practice-driven topic, our comprehensive study goes beyond conventional literature reviews by providing both an overview of existing research and the development of a roofline model. Our first step is to develop a roofline model, which enables us to pinpoint bottlenecks in LLM deployments, allowing researchers to resort to more specific deployment strategies. By meticulously assembling the latest developments in the field, our survey spans an array of pivotal areas, including innovations in weight optimization techniques, enhancements in decoding algorithms, as well as advancements in hardware and system-level optimizations. It is important to note that this project will be updated and maintained.

References

Agarwal, R., Vieillard, N., Stanczyk, P., Ramos, S., Geist, M., and Bachem, O. (2023). Gkd: Generalized knowledge distillation for auto-regressive sequence models. *arXiv preprint arXiv:2306.13649*. 12

Bae, S., Ko, J., Song, H., and Yun, S.-Y. (2023). Fast and robust early-exiting framework for autoregressive language models with synchronized parallel decoding. 14, 15

Baier-Reinio, A. and Sterck, H. D. (2020). N-ode transformer: A depth-adaptive variant of the transformer using neural ordinary differential equations. 13

Brown, T., Mann, B., Ryder, N., Subbiah, M., Kaplan, J. D., Dhariwal, P., Neelakantan, A., Shyam, P., Sastry, G., Askell, A., et al. (2020). Language models are few-shot learners. *Advances in neural information processing systems*, 33:1877–1901. 1, 16

Cai, T., Li, Y., Geng, Z., Peng, H., Lee, J. D., Chen, D., and Dao, T. (2024). Medusa: Simple llm inference acceleration framework with multiple decoding heads. *arXiv preprint arXiv:2401.10774*. 18, 19

Chae, H., Song, Y., Ong, K. T.-i., Kwon, T., Kim, M., Yu, Y., Lee, D., Kang, D., and Yeo, J. (2023). Dialogue chain-of-thought distillation for commonsense-aware conversational agents. *arXiv preprint arXiv:2310.09343*. 12

Chee, J., Cai, Y., Kuleshov, V., and De Sa, C. (2023). Quip: 2-bit quantization of large language models with guarantees. *Advances in Neural Information Processing Systems*. 9

Chen, C., Borgeaud, S., Irving, G., Lespiau, J.-B., Sifre, L., and Jumper, J. (2023a). Accelerating large language model decoding with speculative sampling. *arXiv preprint arXiv:2302.01318*. 17

Chen, Y., Pan, X., Li, Y., Ding, B., and Zhou, J. (2023b). Ee-llm: Large-scale training and inference of early-exit large language models with 3d parallelism. 15

Choi, J., Wang, Z., Venkataramani, S., Chuang, P. I.-J., Srinivasan, V., and Gopalakrishnan, K. (2018). Pact: Parameterized clipping activation for quantized neural networks. *arXiv preprint arXiv:1805.06085*. 8

Chowdhery, A., Narang, S., Devlin, J., Bosma, M., Mishra, G., Roberts, A., Barham, P., Chung, H. W., Sutton, C., Gehrmann, S., Schuh, P., Shi, K., Tsvyashchenko, S., Maynez, J., Rao, A., Barnes, P., Tay, Y., Shazeer, N., Prabhakaran, V., Reif, E., Du, N., Hutchinson, B., Pope, R., Bradbury, J., Austin, J., Isard, M., Gur-Ari, G., Yin, P., Duke, T., Levskaya, A., Ghemawat, S., Dev, S., Michalewski, H., Garcia, X., Misra, V., Robinson, K., Fedus, L., Zhou, D., Ippolito, D., Luan, D., Lim, H., Zoph, B., Spiridonov, A., Sepassi, R., Dohan, D., Agrawal, S., Omernick, M., Dai, A. M., Pillai, T. S., Pellat, M., Lewkowycz, A., Moreira, E., Child, R., Polozov, O., Lee, K., Zhou, Z., Wang, X., Saeta, B., Diaz, M., Firat, O., Catasta, M., Wei, J., Meier-Hellstern, K., Eck, D., Dean, J., Petrov, S., and Fiedel, N. (2022). Palm: Scaling language modeling with pathways. 16

Corro, L. D., Giorno, A. D., Agarwal, S., Yu, B., Awadallah, A., and Mukherjee, S. (2023). Skipdecode: Autoregressive skip decoding with batching and caching for efficient llm inference. 15

Courbariaux, M., Bengio, Y., and David, J.-P. (2015). Binaryconnect: Training deep neural networks with binary weights during propagations. *Advances in neural information processing systems*, 28. 8

de Jong, M., Zemlyanskiy, Y., Ainslie, J., FitzGerald, N., Sanghai, S., Sha, F., and Cohen, W. (2023). Fido: Fusion-in-decoder optimized for stronger performance and faster inference. 13

Dettmers, T., Lewis, M., Belkada, Y., and Zettlemoyer, L. (2022). Llm. int8 (): 8-bit matrix multiplication for transformers at scale. *arXiv preprint arXiv:2208.07339*. 9

Dettmers, T., Pagnoni, A., Holtzman, A., and Zettlemoyer, L. (2023a). Qlora: Efficient finetuning of quantized llms. *arXiv preprint arXiv:2305.14314*. 10

Dettmers, T., Svirschevski, R., Egiazarian, V., Kuznedelev, D., Frantar, E., Ashkboos, S., Borzunov, A., Hoefler, T., and Alistarh, D. (2023b). Spqr: A sparse-quantized representation for near-lossless llm weight compression. *arXiv preprint arXiv:2306.03078*. 9

Dettmers, T. and Zettlemoyer, L. (2023). The case for 4-bit precision: k-bit inference scaling laws. In *International Conference on Machine Learning*, pages 7750–7774. PMLR. 9

Devlin, J., Chang, M.-W., Lee, K., and Toutanova, K. (2019). Bert: Pre-training of deep bidirectional transformers for language understanding. 16

Devvrit, Kudugunta, S., Kusupati, A., Dettmers, T., Chen, K., Dhillon, I., Tsvetkov, Y., Hajishirzi, H., Kakade, S., Farhadi, A., and Jain, P. (2023). Matformer: Nested transformer for elastic inference. 16

Din, A. Y., Karidi, T., Choshen, L., and Geva, M. (2023). Jump to conclusions: Short-cutting transformers with linear transformations. 15

Ding, T., Chen, T., Zhu, H., Jiang, J., Zhong, Y., Zhou, J., Wang, G., Zhu, Z., Zharkov, I., and Liang, L. (2023). The efficiency spectrum of large language models: An algorithmic survey. *arXiv preprint arXiv:2312.00678*. 2, 15

Dong, Z., Yao, Z., Gholami, A., Mahoney, M. W., and Keutzer, K. (2019). Hawq: Hessian aware quantization of neural networks with mixed-precision. In *Proceedings of the IEEE/CVF International Conference on Computer Vision*, pages 293–302. 8

Du, N., Huang, Y., Dai, A. M., Tong, S., Lepikhin, D., Xu, Y., Krikun, M., Zhou, Y., Yu, A. W., Firat, O., et al. (2022). Glam: Efficient scaling of language models with mixture-of-experts. In *International Conference on Machine Learning*, pages 5547–5569. PMLR. 16

Elbayad, M., Gu, J., Grave, E., and Auli, M. (2020). Depth-adaptive transformer. 13, 15

Fedus, W., Dean, J., and Zoph, B. (2022). A review of sparse expert models in deep learning. *arXiv preprint arXiv:2209.01667*. 16

Fedus, W., Zoph, B., and Shazeer, N. (2021). Switch transformers: Scaling to trillion parameter models with simple and efficient sparsity.(2021). *arXiv preprint cs.LG/2101.03961*. 16

Frantar, E. and Alistarh, D. (2023). Sparsegpt: Massive language models can be accurately pruned in one-shot. *ICML*. 11

Frantar, E., Ashkboos, S., Hoefler, T., and Alistarh, D. (2022). Gptq: Accurate post-training quantization for generative pre-trained transformers. *arXiv preprint arXiv:2210.17323*. 9

Fu, Y., Bailis, P., Stoica, I., and Zhang, H. (2023a). Breaking the sequential dependency of llm inference using lookahead decoding. 19

Fu, Y., Peng, H., Ou, L., Sabharwal, A., and Khot, T. (2023b). Specializing smaller language models towards multi-step reasoning. *arXiv preprint arXiv:2301.12726*. 12

Geva, M., Caciularu, A., Wang, K. R., and Goldberg, Y. (2022). Transformer feed-forward layers build predictions by promoting concepts in the vocabulary space. 13

Ghazvininejad, M., Levy, O., Liu, Y., and Zettlemoyer, L. (2019). Mask-predict: Parallel decoding of conditional masked language models. 19

Gholami, A., Kim, S., Dong, Z., Yao, Z., Mahoney, M. W., and Keutzer, K. (2022). A survey of quantization methods for efficient neural network inference. In *Low-Power Computer Vision*, pages 291–326. Chapman and Hall/CRC. 6

Gou, J., Yu, B., Maybank, S. J., and Tao, D. (2021). Knowledge distillation: A survey. *International Journal of Computer Vision*, 129:1789–1819. 11

Gu, J., Bradbury, J., Xiong, C., Li, V. O., and Socher, R. (2017). Non-autoregressive neural machine translation. *arXiv preprint arXiv:1711.02281*. 19

Gu, J. and Kong, X. (2020). Fully non-autoregressive neural machine translation: Tricks of the trade. 19

Gu, Y., Dong, L., Wei, F., and Huang, M. (2023). Knowledge distillation of large language models. *arXiv preprint arXiv:2306.08543*. 12

Guo, C., Tang, J., Hu, W., Leng, J., Zhang, C., Yang, F., Liu, Y., Guo, M., and Zhu, Y. (2023a). Olive: Accelerating large language models via hardware-friendly outlier-victim pair quantization. In *Proceedings of the 50th Annual International Symposium on Computer Architecture*, pages 1–15. 9

Guo, H., Greengard, P., Xing, E. P., and Kim, Y. (2023b). Lq-lora: Low-rank plus quantized matrix decomposition for efficient language model finetuning. *arXiv preprint arXiv:2311.12023*. 10

Guo, J., Xu, L., and Chen, E. (2020). Jointly masked sequence-to-sequence model for non-autoregressive neural machine translation. In Jurafsky, D., Chai, J., Schluter, N., and Tetreault, J., editors, *Proceedings of the 58th Annual Meeting of the Association for Computational Linguistics*, pages 376–385, Online. Association for Computational Linguistics. 19

Guo, S., Xu, J., Zhang, L. L., and Yang, M. (2023c). Compresso: Structured pruning with collaborative prompting learns compact large language models. *arXiv preprint arXiv:2310.05015*. 11

He, Z., Zhong, Z., Cai, T., Lee, J. D., and He, D. (2023). Rest: Retrieval-based speculative decoding. *arXiv preprint arXiv:2311.08252*. 19

Hinton, G., Vinyals, O., and Dean, J. (2015). Distilling the knowledge in a neural network. *arXiv preprint arXiv:1503.02531*. 11

Hoffmann, J., Borgeaud, S., Mensch, A., Buchatskaya, E., Cai, T., Rutherford, E., de Las Casas, D., Hendricks, L. A., Welbl, J., Clark, A., Hennigan, T., Noland, E., Millican, K., van den Driessche, G., Damoc, B., Guy, A., Osindero, S., Simonyan, K., Elsen, E., Rae, J. W., Vinyals, O., and Sifre, L. (2022). Training compute-optimal large language models. 16

Hou, L., Huang, Z., Shang, L., Jiang, X., Chen, X., and Liu, Q. (2020). Dynabert: Dynamic bert with adaptive width and depth. 13

Hsieh, C.-Y., Li, C.-L., Yeh, C.-K., Nakhost, H., Fujii, Y., Ratner, A., Krishna, R., Lee, C.-Y., and Pfister, T. (2023). Distilling step-by-step! outperforming larger language models with less training data and smaller model sizes. *arXiv preprint arXiv:2305.02301*. 12

Hu, E. J., Shen, Y., Wallis, P., Allen-Zhu, Z., Li, Y., Wang, S., Wang, L., and Chen, W. (2021). Lora: Low-rank adaptation of large language models. *arXiv preprint arXiv:2106.09685*. 10

Hu, Z., Lan, Y., Wang, L., Xu, W., Lim, E.-P., Lee, R. K.-W., Bing, L., and Poria, S. (2023). Llm-adapters: An adapter family for parameter-efficient fine-tuning of large language models. *arXiv preprint arXiv:2304.01933*. 10

Huang, W., Liu, Y., Qin, H., Li, Y., Zhang, S., Liu, X., Magno, M., and Qi, X. (2024). Billm: Pushing the limit of post-training quantization for llms. *arXiv preprint arXiv:2402.04291*. 9

Huang, Y., Chen, Y., Yu, Z., and McKeown, K. (2022). In-context learning distillation: Transferring few-shot learning ability of pre-trained language models. *arXiv preprint arXiv:2212.10670*. 12

Hubara, I., Courbariaux, M., Soudry, D., El-Yaniv, R., and Bengio, Y. (2016). Binarized neural networks. *Advances in neural information processing systems*, 29. 9

Jawahar, G., Mukherjee, S., Liu, X., Kim, Y. J., Mageed, M. A., Laks Lakshmanan, V., Hassan, A., Bubeck, S., and Gao, J. (2023). Automoe: Heterogeneous mixture-of-experts with adaptive computation for efficient neural machine translation.

In *Findings of the Association for Computational Linguistics: ACL 2023*, pages 9116–9132. 17

Ji, Y., Wang, J., Li, J., Chen, Q., Chen, W., and Zhang, M. (2023). Early exit with disentangled representation and equiangular tight frame. In Rogers, A., Boyd-Graber, J., and Okazaki, N., editors, *Findings of the Association for Computational Linguistics: ACL 2023*, pages 14128–14142, Toronto, Canada. Association for Computational Linguistics. 15

Jiang, A. Q., Sablayrolles, A., Roux, A., Mensch, A., Savary, B., Bamford, C., Chaplot, D. S., Casas, D. d. l., Hanna, E. B., Bressand, F., et al. (2024). Mixtral of experts. *arXiv preprint arXiv:2401.04088*. 16

Jiang, Y., Chan, C., Chen, M., and Wang, W. (2023). Lion: Adversarial distillation of closed-source large language model. *arXiv preprint arXiv:2305.12870*. 12

Kaplan, J., McCandlish, S., Henighan, T., Brown, T. B., Chess, B., Child, R., Gray, S., Radford, A., Wu, J., and Amodei, D. (2020). Scaling laws for neural language models. 16

Kim, J., Lee, J. H., Kim, S., Park, J., Yoo, K. M., Kwon, S. J., and Lee, D. (2023a). Memory-efficient fine-tuning of compressed large language models via sub-4-bit integer quantization. *arXiv preprint arXiv:2305.14152*. 10

Kim, M., Lee, S., Lee, J., Hong, S., Chang, D.-S., Sung, W., and Choi, J. (2023b). Token-scaled logit distillation for ternary weight generative language models. *arXiv preprint arXiv:2308.06744*. 8

Kim, S., Hooper, C., Gholami, A., Dong, Z., Li, X., Shen, S., Mahoney, M. W., and Keutzer, K. (2023c). Squeezellm: Dense-and-sparse quantization. *arXiv preprint arXiv:2306.07629*. 9

Kim, S., Hooper, C., Wattanawong, T., Kang, M., Yan, R., Genc, H., Dinh, G., Huang, Q., Keutzer, K., Mahoney, M. W., Shao, Y. S., and Gholami, A. (2023d). Full stack optimization of transformer inference: a survey. 13

Kim, S., Mangalam, K., Moon, S., Malik, J., Mahoney, M. W., Gholami, A., and Keutzer, K. (2023e). Speculative decoding with big little decoder. 17

Kishore Kumar, N. and Schneider, J. (2017). Literature survey on low rank approximation of matrices. *Linear and Multilinear Algebra*, 65(11):2212–2244. 12

Kossmann, F., Jia, Z., and Aiken, A. (2022). Optimizing mixture of experts using dynamic recompilations. *arXiv preprint arXiv:2205.01848*. 17

Lan, T., Cai, D., Wang, Y., Huang, H., and Mao, X.-L. (2023). Copy is all you need. 19

LeCun, Y., Denker, J., and Solla, S. (1989). Optimal brain damage. *Advances in neural information processing systems*, 2. 11

Lee, C., Jin, J., Kim, T., Kim, H., and Park, E. (2023). Owq: Lessons learned from activation outliers for weight quantization in large language models. *arXiv preprint arXiv:2306.02272*. 9

Lee, J., Mansimov, E., and Cho, K. (2018). Deterministic non-autoregressive neural sequence modeling by iterative refinement. 19

Lee-Thorp, J. and Ainslie, J. (2022). Sparse mixers: Combining moe and mixing to build a more efficient bert. *arXiv preprint arXiv:2205.12399*. 16

Lepikhin, D., Lee, H., Xu, Y., Chen, D., Firat, O., Huang, Y., Krikun, M., Shazeer, N., and Chen, Z. (2020). Gshard: Scaling giant models with conditional computation and automatic sharding. *arXiv preprint arXiv:2006.16668*. 16

Leviathan, Y., Kalman, M., and Matias, Y. (2023). Fast inference from transformers via speculative decoding. 17

Li, L., Li, Q., Zhang, B., and Chu, X. (2023a). Norm tweaking: High-performance low-bit quantization of large language models. *arXiv preprint arXiv:2309.02784*. 9

Li, L., Lin, Y., Chen, D., Ren, S., Li, P., Zhou, J., and Sun, X. (2021). Cascadebert: Accelerating inference of pre-trained language models via calibrated complete models cascade. 13

Li, L. H., Hessel, J., Yu, Y., Ren, X., Chang, K.-W., and Choi, Y. (2023b). Symbolic chain-of-thought distillation: Small models can also" think" step-by-step. *arXiv preprint arXiv:2306.14050*. 12

Li, Q., Zhang, Y., Li, L., Yao, P., Zhang, B., Chu, X., Sun, Y., Du, L., and Xie, Y. (2023c). Fptq: Fine-grained post-training quantization for large language models. *arXiv preprint arXiv:2308.15987*. 10

Li, Y., Wei, F., Zhang, C., and Zhang, H. (2024). Eagle: Speculative sampling requires rethinking feature uncertainty. *arXiv preprint arXiv:2401.15077*. 18

Li, Y., Yu, Y., Liang, C., He, P., Karampatziakis, N., Chen, W., and Zhao, T. (2023d). Loftq: Lora-fine-tuning-aware quantization for large language models. *arXiv preprint arXiv:2310.08659*. 10

Li, Z., Lin, Z., He, D., Tian, F., Qin, T., Wang, L., and Liu, T.-Y. (2019). Hint-based training for non-autoregressive machine translation. *arXiv preprint arXiv:1909.06708*. 19

Li, Z., Liu, X., Zhu, B., Dong, Z., Gu, Q., and Keutzer, K. (2023e). Qft: Quantized full-parameter tuning of llms with affordable resources. *arXiv preprint arXiv:2310.07147*. 10

Liang, C., Jiang, H., Li, Z., Tang, X., Yin, B., and Zhao, T. (2023a). Homodistil: Homotopic task-agnostic distillation of pre-trained transformers. *arXiv preprint arXiv:2302.09632*. 12

Liang, C., Zuo, S., Zhang, Q., He, P., Chen, W., and Zhao, T. (2023b). Less is more: Task-aware layer-wise distillation for language model compression. In *International Conference on Machine Learning*, pages 20852–20867. PMLR. 12

Liang, T., Glossner, J., Wang, L., Shi, S., and Zhang, X. (2021). Pruning and quantization for deep neural network acceleration: A survey. *Neurocomputing*, 461:370–403. 11

Lin, J., Tang, J., Tang, H., Yang, S., Dang, X., and Han, S. (2023). Awq: Activation-aware weight quantization for llm compression and acceleration. *arXiv preprint arXiv:2306.00978*. 9

Liu, M., Zeng, A., Wang, B., Zhang, P., Tang, J., and Dong, Y. (2024). Apar: Llms can do auto-parallel auto-regressive decoding. 19

Liu, W., Zhou, P., Zhao, Z., Wang, Z., Deng, H., and Ju, Q. (2020). Fastbert: a self-distilling bert with adaptive inference time. 13

Liu, X., Hu, L., Bailis, P., Stoica, I., Deng, Z., Cheung, A., and Zhang, H. (2023a). Online speculative decoding. *arXiv preprint arXiv:2310.07177*. 18

Liu, X., Sun, T., He, J., Wu, J., Wu, L., Zhang, X., Jiang, H., Cao, Z., Huang, X., and Qiu, X. (2022). Towards efficient NLP: A standard evaluation and a strong baseline. In Carpuat, M., de Marneffe, M.-C., and Meza Ruiz, I. V., editors, *Proceedings of the 2022 Conference of the North American Chapter of the Association for Computational Linguistics: Human Language Technologies*, pages 3288–3303, Seattle, United States. Association for Computational Linguistics. 13

Liu, Z., Oguz, B., Zhao, C., Chang, E., Stock, P., Mehdad, Y., Shi, Y., Krishnamoorthi, R., and Chandra, V. (2023b). Llm-qat: Data-free quantization aware training for large language models. *arXiv preprint arXiv:2305.17888*. 8

Liu, Z., Wang, J., Dao, T., Zhou, T., Yuan, B., Song, Z., Shrivastava, A., Zhang, C., Tian, Y., Re, C., and Chen, B. (2023c). Deja vu: Contextual sparsity for efficient llms at inference time. 15

Ma, X., Fang, G., and Wang, X. (2023). Llm-pruner: On the structural pruning of large language models. *arXiv preprint arXiv:2305.11627*. 11

Miao, X., Oliaro, G., Zhang, Z., Cheng, X., Jin, H., Chen, T., and Jia, Z. (2023a). Towards efficient generative large language model serving: A survey from algorithms to systems. *arXiv preprint arXiv:2312.15234*. 2

Miao, X., Oliaro, G., Zhang, Z., Cheng, X., Wang, Z., Wong, R. Y. Y., Chen, Z., Arfeen, D., Abhyankar, R., and Jia, Z. (2023b). Specinfer: Accelerating generative llm serving with speculative inference and token tree verification. *arXiv preprint arXiv:2305.09781*. 17, 18

Monea, G., Joulin, A., and Grave, E. (2023). Pass: Parallel speculative sampling. *arXiv preprint arXiv:2311.13581*. 18

Ning, X., Lin, Z., Zhou, Z., Wang, Z., Yang, H., and Wang, Y. (2023). Skeleton-of-thought: Large language models can do parallel decoding. 19

OpenAI, :, Achiam, J., Adler, S., Agarwal, S., Ahmad, L., Akkaya, I., Aleman, F. L., Almeida, D., Altenschmidt, J., Altman, S., Anadkat, S., Avila, R., Babuschkin, I., Balaji, S., Balcom, V., Baltescu, P., Bao, H., Bavarian, M., Belgum, J., Bello, I., Berdine, J., Bernadett-Shapiro, G., Berner, C., Bogdonoff, L., Boiko, O., Boyd, M., Brakman, A.-L., Brockman, G., Brooks, T., Brundage, M., Button, K., Cai, T., Campbell, R., Cann, A., Carey, B., Carlson, C., Carmichael, R., Chan, B., Chang, C., Chantzis, F., Chen, D., Chen, S., Chen, R., Chen, J., Chen, M., Chess, B., Cho, C., Chu, C., Chung, H. W., Cummings, D., Currier, J., Dai, Y., Decareaux, C., Degry, T., Deutsch, N., Deville, D., Dhar, A., Dohan, D., Dowling, S., Dunning, S., Ecoffet, A., Eleti, A., Eloundou, T., Farhi, D., Fedus, L., Felix, N., Fishman, S. P., Forte, J., Fulford, I., Gao, L., Georges, E., Gibson, C., Goel, V., Gogineni, T., Goh, G., Gontijo-Lopes, R., Gordon, J., Grafstein, M., Gray, S., Greene, R., Gross, J., Gu, S. S., Guo, Y., Hallacy, C., Han, J., Harris, J., He, Y., Heaton, M., Heidecke, J., Hesse, C., Hickey, A., Hickey, W., Hoeschele, P., Houghton, B., Hsu, K., Hu, S., Hu, X., Huizinga, J., Jain, S., Jain, S., Jang, J., Jiang, A., Jiang, R., Jin, H., Jin, D., Jomoto, S., Jonn, B., Jun, H., Kaftan, T., Łukasz Kaiser, Kamali, A., Kanitscheider, I., Keskar, N. S., Khan, T., Kilpatrick, L., Kim, J. W., Kim, C., Kim, Y., Kirchner, H., Kiros, J., Knight, M., Kokotajlo, D., Łukasz Kondraciuk, Kondrich, A., Konstantinidis, A., Kosic, K., Krueger, G., Kuo, V., Lampe, M., Lan, I., Lee, T., Leike, J., Leung, J., Levy, D., Li, C. M., Lim, R., Lin, M., Lin, S., Litwin, M., Lopez, T., Lowe, R., Lue, P., Makanju, A., Malfacini, K., Manning, S., Markov, T., Markovski, Y., Martin, B., Mayer, K., Mayne, A., McGrew, B., McKinney, S. M., McLeavey, C., McMillan, P., McNeil, J., Medina, D., Mehta, A., Menick, J., Metz, L., Mishchenko, A., Mishkin, P., Monaco, V., Morikawa, E., Mossing, D., Mu, T., Murati, M., Murk, O., Mély, D., Nair, A., Nakano, R., Nayak, R., Neelakantan, A., Ngo, R., Noh, H., Ouyang, L., O'Keefe, C., Pachocki, J., Paino, A., Palermo, J., Pantuliano, A., Parascandolo, G., Parish, J., Parparita, E., Passos, A., Pavlov, M., Peng, A., Perelman, A., de Avila Belbute Peres, F., Petrov, M., de Oliveira Pinto, H. P., Michael, Pokorny, Pokrass, M., Pong, V., Powell, T., Power, A., Power, B., Proehl, E., Puri, R., Radford, A., Rae, J., Ramesh, A., Raymond, C., Real, F., Rimbach, K., Ross, C., Rotsted, B., Roussez, H., Ryder, N., Saltarelli, M., Sanders, T., Santurkar, S., Sastry, G., Schmidt, H., Schnurr, D., Schulman, J., Selsam, D., Sheppard, K., Sherbakov, T., Shieh, J., Shoker, S., Shyam, P., Sidor, S., Sigler, E., Simens, M., Sitkin, J., Slama, K., Sohl, I., Sokolowsky, B., Song, Y., Staudacher, N., Such, F. P., Summers, N., Sutskever, I., Tang, J., Tezak, N., Thompson, M., Tillet, P., Tootoonchian, A., Tseng, E., Tuggle, P., Turley, N., Tworek, J., Uribe, J. F. C., Vallone, A., Vijayvergiya, A., Voss, C., Wainwright, C., Wang, J. J., Wang, A., Wang, B., Ward, J., Wei, J., Weinmann, C., Welihinda, A., Welinder, P., Weng, J., Weng, L., Wiethoff, M., Willner, D., Winter, C., Wolrich, S., Wong, H., Workman, L., Wu, S., Wu, J., Wu, M., Xiao, K., Xu, T., Yoo, S., Yu, K., Yuan, Q., Zaremba, W., Zellers, R., Zhang, C., Zhang, M., Zhao, S., Zheng, T., Zhuang, J., Zhuk, W., and Zoph, B. (2023). Gpt-4 technical report. 13

Ortega, J. M. and Rheinboldt, W. C. (2000). *Iterative solution of nonlinear equations in several variables*. SIAM. 19

Oseledets, I. V. (2011). Tensor-train decomposition. *SIAM Journal on Scientific Computing*, 33(5):2295–2317. 13

Ouyang, L., Wu, J., Jiang, X., Almeida, D., Wainwright, C., Mishkin, P., Zhang, C., Agarwal, S., Slama, K., Ray, A., et al. (2022). Training language models to follow instructions with

human feedback. *Advances in Neural Information Processing Systems*, 35:27730–27744. 1

Park, G., Park, B., Kim, M., Lee, S., Kim, J., Kwon, B., Kwon, S. J., Kim, B., Lee, Y., and Lee, D. (2023). Lut-gemm: Quantized matrix multiplication based on luts for efficient inference in large-scale generative language models. *arXiv preprint arXiv:2206.09557*. 9

Rajbhandari, S., Li, C., Yao, Z., Zhang, M., Aminabadi, R. Y., Awan, A. A., Rasley, J., and He, Y. (2022). Deepspeed-moe: Advancing mixture-of-experts inference and training to power next-generation ai scale. In *International Conference on Machine Learning*, pages 18332–18346. PMLR. 17

Rotem, D., Hassid, M., Mamou, J., and Schwartz, R. (2023). Finding the sweet spot: Analysis and improvement of adaptive inference in low resource settings. 15

Sahu, G., Vechtomova, O., Bahdanau, D., and Laradji, I. H. (2023). Promptmix: A class boundary augmentation method for large language model distillation. *arXiv preprint arXiv:2310.14192*. 12

Santilli, A., Severino, S., Postolache, E., Maiorca, V., Mancusi, M., Marin, R., and Rodolà, E. (2023). Accelerating transformer inference for translation via parallel decoding. *arXiv preprint arXiv:2305.10427*. 19

Savinov, N., Chung, J., Binkowski, M., Elsen, E., and Oord, A. v. d. (2021). Step-unrolled denoising autoencoders for text generation. *arXiv preprint arXiv:2112.06749*. 19, 20

Scao, T. L., Fan, A., Akiki, C., Pavlick, E., Ilić, S., Hesslow, D., Castagné, R., Luccioni, A. S., Yvon, F., Gallé, M., et al. (2022). Bloom: A 176b-parameter open-access multilingual language model. *arXiv preprint arXiv:2211.05100*. 1

Schotthöfer, S., Zangrando, E., Kusch, J., Ceruti, G., and Tudisco, F. (2022). Low-rank lottery tickets: finding efficient low-rank neural networks via matrix differential equations. *Advances in Neural Information Processing Systems*, 35:20051–20063. 12

Schuster, T., Fisch, A., Gupta, J., Dehghani, M., Bahri, D., Tran, V. Q., Tay, Y., and Metzler, D. (2022). Confident adaptive language modeling. 14, 15

Schuster, T., Fisch, A., Jaakkola, T., and Barzilay, R. (2021). Consistent accelerated inference via confident adaptive transformers. 13

Schwartz, R., Stanovsky, G., Swayamdipta, S., Dodge, J., and Smith, N. A. (2020). The right tool for the job: Matching model and instance complexities. In Jurafsky, D., Chai, J., Schluter, N., and Tetreault, J., editors, *Proceedings of the 58th Annual Meeting of the Association for Computational Linguistics*, pages 6640–6651, Online. Association for Computational Linguistics. 13

Shang, Y., Duan, B., Zong, Z., Nie, L., and Yan, Y. (2021). Lipschitz continuity guided knowledge distillation. In *Proceedings of the IEEE/CVF International Conference on Computer Vision*, pages 10675–10684. 11

Shang, Y., Yuan, Z., Wu, Q., and Dong, Z. (2023). Pb-llm: Partially binarized large language models. In *ICLR*. 8, 9

Shao, C., Zhang, J., Feng, Y., Meng, F., and Zhou, J. (2020). Minimizing the bag-of-ngrams difference for non-autoregressive neural machine translation. In *Proceedings of the AAAI conference on artificial intelligence*, volume 34, pages 198–205. 19

Sharma, P., Ash, J. T., and Misra, D. (2023). The truth is in there: Improving reasoning in language models with layer-selective rank reduction. *arXiv preprint arXiv:2312.13558*. 13

Simoulin, A. and Crabbé, B. (2021). How many layers and why? An analysis of the model depth in transformers. In Kabbara, J., Lin, H., Paullada, A., and Vamvas, J., editors, *Proceedings of the 59th Annual Meeting of the Association for Computational Linguistics and the 11th International Joint Conference on Natural Language Processing: Student Research Workshop*, pages 221–228, Online. Association for Computational Linguistics. 13

Song, Y., Meng, C., Liao, R., and Ermon, S. (2021). Accelerating feedforward computation via parallel nonlinear equation solving. In Meila, M. and Zhang, T., editors, *Proceedings of the 38th International Conference on Machine Learning*, volume 139 of *Proceedings of Machine Learning Research*, pages 9791–9800. PMLR. 19

Song, Y., Mi, Z., Xie, H., and Chen, H. (2023). Powerinfer: Fast large language model serving with a consumer-grade gpu. 15

Stern, M., Shazeer, N., and Uszkoreit, J. (2018). Blockwise parallel decoding for deep autoregressive models. *Advances in Neural Information Processing Systems*, 31. 18

Stickland, A. C. and Murray, I. (2019). Bert and pals: Projected attention layers for efficient adaptation in multi-task learning. 13

Sun, M., Liu, Z., Bair, A., and Kolter, J. Z. (2023a). A simple and effective pruning approach for large language models. *arXiv preprint arXiv:2306.11695*. 11

Sun, Z., Li, Z., Wang, H., He, D., Lin, Z., and Deng, Z. (2019). Fast structured decoding for sequence models. *Advances in Neural Information Processing Systems*, 32. 19

Sun, Z., Suresh, A. T., Ro, J. H., Beirami, A., Jain, H., and Yu, F. (2023b). Spectr: Fast speculative decoding via optimal transport. *arXiv preprint arXiv:2310.15141*. 17

Touvron, H., Lavril, T., Izacard, G., Martinet, X., Lachaux, M.-A., Lacroix, T., Rozière, B., Goyal, N., Hambro, E., Azhar, F., et al. (2023a). Llama: Open and efficient foundation language models. *arXiv preprint arXiv:2302.13971*. 1, 7

Touvron, H., Martin, L., Stone, K., Albert, P., Almahairi, A., Babaei, Y., Bashlykov, N., Batra, S., Bhargava, P., Bhosale, S., Bikel, D., Blecher, L., Ferrer, C. C., Chen, M., Cucurull, G., Esiobu, D., Fernandes, J., Fu, J., Fu, W., Fuller, B., Gao, C., Goswami, V., Goyal, N., Hartshorn, A., Hosseini, S., Hou,

R., Inan, H., Kardas, M., Kerkez, V., Khabsa, M., Kloumann, I., Korenev, A., Koura, P. S., Lachaux, M.-A., Lavril, T., Lee, J., Liskovich, D., Lu, Y., Mao, Y., Martinet, X., Mihaylov, T., Mishra, P., Molybog, I., Nie, Y., Poulton, A., Reizenstein, J., Rungta, R., Saladi, K., Schelten, A., Silva, R., Smith, E. M., Subramanian, R., Tan, X. E., Tang, B., Taylor, R., Williams, A., Kuan, J. X., Xu, P., Yan, Z., Zarov, I., Zhang, Y., Fan, A., Kambadur, M., Narang, S., Rodriguez, A., Stojnic, R., Edunov, S., and Scialom, T. (2023b). Llama 2: Open foundation and fine-tuned chat models. 16

Touvron, H., Martin, L., Stone, K., Albert, P., Almahairi, A., Babaei, Y., Bashlykov, N., Batra, S., Bhargava, P., Bhosale, S., et al. (2023c). Llama 2: Open foundation and fine-tuned chat models. *arXiv preprint arXiv:2307.09288*. 1

Valipour, M., Rezagholizadeh, M., Kobyzev, I., and Ghodsi, A. (2022). Dylora: Parameter efficient tuning of pre-trained models using dynamic search-free low-rank adaptation. *arXiv preprint arXiv:2210.07558*. 10

Wang, P., Wang, Z., Li, Z., Gao, Y., Yin, B., and Ren, X. (2023). Scott: Self-consistent chain-of-thought distillation. *arXiv preprint arXiv:2305.01879*. 12

Wang, W., Chen, W., Luo, Y., Long, Y., Lin, Z., Zhang, L., Lin, B., Cai, D., and He, X. (2024). Model compression and efficient inference for large language models: A survey. *arXiv preprint arXiv:2402.09748*. 2

Wang, Y., Tian, F., He, D., Qin, T., Zhai, C., and Liu, T.-Y. (2019). Non-autoregressive machine translation with auxiliary regularization. In *Proceedings of the AAAI conference on artificial intelligence*, volume 33, pages 5377–5384. 19

Wei, B., Wang, M., Zhou, H., Lin, J., Xie, J., and Sun, X. (2019). Imitation learning for non-autoregressive neural machine translation. *arXiv preprint arXiv:1906.02041*. 19

Wu, M., Waheed, A., Zhang, C., Abdul-Mageed, M., and Aji, A. F. (2023a). Lamini-lm: A diverse herd of distilled models from large-scale instructions. *arXiv preprint arXiv:2304.14402*. 12

Wu, S., Chen, H., Quan, X., Wang, Q., and Wang, R. (2023b). Ad-kd: Attribution-driven knowledge distillation for language model compression. *arXiv preprint arXiv:2305.10010*. 12

Wu, X., Yao, Z., and He, Y. (2023c). Zeroquant-fp: A leap forward in llms post-training w4a8 quantization using floating-point formats. *arXiv preprint arXiv:2307.09782*. 9

Xia, H., Zheng, Z., Li, Y., Zhuang, D., Zhou, Z., Qiu, X., Li, Y., Lin, W., and Song, S. L. (2023a). Flash-llm: Enabling cost-effective and highly-efficient large generative model inference with unstructured sparsity. *arXiv preprint arXiv:2309.10285*. 11

Xia, M., Gao, T., Zeng, Z., and Chen, D. (2023b). Sheared llama: Accelerating language model pre-training via structured pruning. *arXiv preprint arXiv:2310.06694*. 11

Xiao, G., Lin, J., Seznec, M., Wu, H., Demouth, J., and Han, S. (2023a). Smoothquant: Accurate and efficient post-training quantization for large language models. In *International Conference on Machine Learning*, pages 38087–38099. PMLR. 9

Xiao, Y., Wu, L., Guo, J., Li, J., Zhang, M., Qin, T., and Liu, T.-y. (2023b). A survey on non-autoregressive generation for neural machine translation and beyond. *IEEE Transactions on Pattern Analysis and Machine Intelligence*. 19

Xin, J., Tang, R., Lee, J., Yu, Y., and Lin, J. (2020). Deebert: Dynamic early exiting for accelerating bert inference. 13

Xu, D., Yin, W., Jin, X., Zhang, Y., Wei, S., Xu, M., and Liu, X. (2023a). Llmcad: Fast and scalable on-device large language model inference. *arXiv preprint arXiv:2309.04255*. 17, 18

Xu, M., Xu, Y. L., and Mandic, D. P. (2023b). Tensorgpt: Efficient compression of the embedding layer in llms based on the tensor-train decomposition. *arXiv preprint arXiv:2307.00526*. 13

Xu, X., Li, M., Tao, C., Shen, T., Cheng, R., Li, J., Xu, C., Tao, D., and Zhou, T. (2024). A survey on knowledge distillation of large language models. 11

Xu, Y., Xie, L., Gu, X., Chen, X., Chang, H., Zhang, H., Chen, Z., Zhang, X., and Tian, Q. (2023c). Qa-lora: Quantization-aware low-rank adaptation of large language models. *arXiv preprint arXiv:2309.14717*. 10

Yang, N., Ge, T., Wang, L., Jiao, B., Jiang, D., Yang, L., Majumder, R., and Wei, F. (2023). Inference with reference: Lossless acceleration of large language models. *arXiv preprint arXiv:2304.04487*. 19

Yao, Z., Yazdani Aminabadi, R., Zhang, M., Wu, X., Li, C., and He, Y. (2022). Zeroquant: Efficient and affordable post-training quantization for large-scale transformers. *Advances in Neural Information Processing Systems*, 35:27168–27183. 9

Yi, R., Guo, L., Wei, S., Zhou, A., Wang, S., and Xu, M. (2023). Edgemoe: Fast on-device inference of moe-based large language models. *arXiv preprint arXiv:2308.14352*. 17

Yin, L., Wu, Y., Zhang, Z., Hsieh, C.-Y., Wang, Y., Jia, Y., Pechenizkiy, M., Liang, Y., Wang, Z., and Liu, S. (2023). Outlier weighed layerwise sparsity (owl): A missing secret sauce for pruning llms to high sparsity. *arXiv preprint arXiv:2310.05175*. 11

Yuan, Z., Niu, L., Liu, J., Liu, W., Wang, X., Shang, Y., Sun, G., Wu, Q., Wu, J., and Wu, B. (2023a). Rptq: Reorder-based post-training quantization for large language models. *arXiv preprint arXiv:2304.01089*. 9

Yuan, Z., Shang, Y., Song, Y., Wu, Q., Yan, Y., and Sun, G. (2023b). Asvd: Activation-aware singular value decomposition for compressing large language models. *arXiv preprint arXiv:2312.05821*. 13

Yue, Y., Yuan, Z., Duanmu, H., Zhou, S., Wu, J., and Nie, L. (2024). Wkvquant: Quantizing weight and key/value cache for large language models gains more. *arXiv preprint arXiv:2402.12065*. 10

Yuksel, S. E., Wilson, J. N., and Gader, P. D. (2012). Twenty years of mixture of experts. *IEEE Transactions on Neural Networks and Learning Systems*, 23(8):1177–1193. 16

Zeng, Z., Hong, Y., Dai, H., Zhuang, H., and Chen, C. (2023). Consistentee: A consistent and hardness-guided early exiting method for accelerating language models inference. 14, 15

Zhang, J., Wang, J., Li, H., Shou, L., Chen, K., Chen, G., and Mehrotra, S. (2023). Draft & verify: Lossless large language model acceleration via self-speculative decoding. *arXiv preprint arXiv:2309.08168*. 18

Zhang, S., Roller, S., Goyal, N., Artetxe, M., Chen, M., Chen, S., Dewan, C., Diab, M., Li, X., Lin, X. V., et al. (2022). Opt: Open pre-trained transformer language models. *arXiv preprint arXiv:2205.01068*. 1

Zhao, W. X., Zhou, K., Li, J., Tang, T., Wang, X., Hou, Y., Min, Y., Zhang, B., Zhang, J., Dong, Z., et al. (2023). A survey of large language models. *arXiv preprint arXiv:2303.18223*. 1, 3

Zhou, W., Xu, C., Ge, T., McAuley, J., Xu, K., and Wei, F. (2020). Bert loses patience: Fast and robust inference with early exit. 13

Zhou, Y., Lyu, K., Rawat, A. S., Menon, A. K., Rostamizadeh, A., Kumar, S., Kagy, J.-F., and Agarwal, R. (2023). Distillspec: Improving speculative decoding via knowledge distillation. *arXiv preprint arXiv:2310.08461*. 18

Zhu, W. (2021). LeeBERT: Learned early exit for BERT with cross-level optimization. In Zong, C., Xia, F., Li, W., and Navigli, R., editors, *Proceedings of the 59th Annual Meeting of the Association for Computational Linguistics and the 11th International Joint Conference on Natural Language Processing (Volume 1: Long Papers)*, pages 2968–2980, Online. Association for Computational Linguistics. 13

Zhu, X., Li, J., Liu, Y., Ma, C., and Wang, W. (2023). A survey on model compression for large language models. *arXiv preprint arXiv:2308.07633*. 2

Zoph, B., Bello, I., Kumar, S., Du, N., Huang, Y., Dean, J., Shazeer, N., and Fedus, W. (2022). St-moe: Designing stable and transferable sparse expert models. *arXiv preprint arXiv:2202.08906*. 16